Earth, Planets and Space

2016 Kumamoto Earthquake Sequence and Its Impact on Earthquake Science and Hazard Assessment

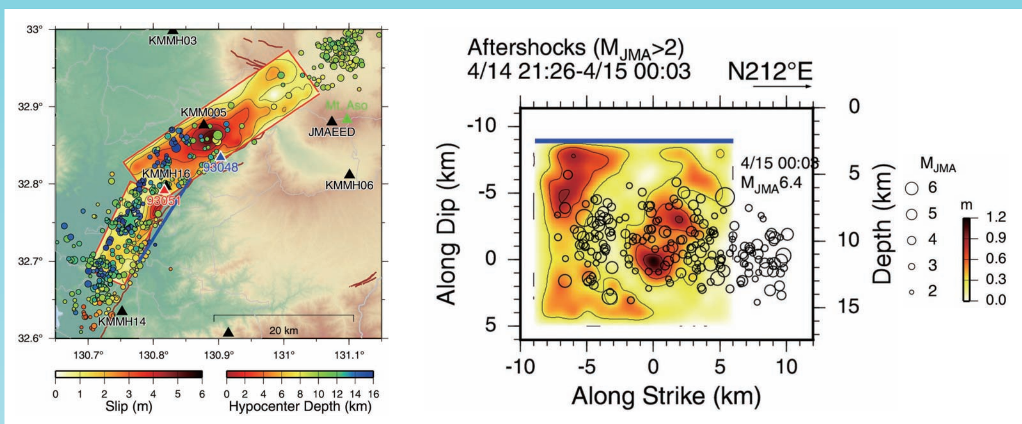

Society of Geomagnetism and Earth, Planetary and Space Sciences (SGEPSS)
The Seismological Society of Japan
The Volcanological Society of Japan
The Geodetic Society of Japan
The Japanese Society for Planetary Sciences

Japan Geoscience Union
Springer Open

Journal Scope

Earth, Planets and Space (EPS) is the official journal of the Society of Geomagnetism and Earth, Planetary and Space Sciences, The Seismological Society of Japan, The Volcanological Society of Japan, The Geodetic Society of Japan, and The Japanese Society for Planetary Sciences.
EPS is a peer-reviewed, open-access journal published under SpringerOpen. It is an international journal covering scientific articles in the entire field of earth and planetary sciences, particularly geomagnetism, aeronomy, space science, seismology, volcanology, geodesy, and planetary science. EPS also welcomes articles in new and interdisciplinary subjects, and technical reports on instrumentation and software.

The journal was launched in 1998 and has since published over 3000 articles. All of them are available for free on SpringerLink:

http://link.springer.com/journal/40623

More information about the journal, its article collections, and the submission process is available on the journal homepage:

http://earth-planets-space.springeropen.com

Submit your next research article to Earth, Planets and Space via:

https://www.editorialmanager.com/epsp

Yours sincerely,

Prof. Yasuo Ogawa
Editor-in-Chief, *Earth, Planets and Space*
editor-in-chief@earth-planets-space.org

Earth, Planets and Space

Hashimoto *et al. Earth, Planets and Space* (2017) 69:98
DOI 10.1186/s40623-017-0682-7

PREFACE

Open Access

Special issue "2016 Kumamoto earthquake sequence and its impact on earthquake science and hazard assessment"

Manabu Hashimoto[1*], Martha Savage[2], Takuya Nishimura[1], Haruo Horikawa[3] and Hiroyuki Tsutsumi[4]

The Kumamoto earthquake sequence that started on April 15, 2016, resulted in more than 60 fatalities and brought about serious damage to Kumamoto Prefecture. It is the first time that the seismic intensity of 7 (on the Japan Meteorological Agency scale) was recorded twice within 2 days, which unnerved the population in the affected areas and made the response difficult. Furthermore, seismicity spread out across Kyushu Island, which enhanced uneasiness in society. The earthquakes occurred on known active faults where long-term probability of earthquake occurrence was disseminated, but such complex activity was unexpected. This unique sequence will clearly have a significant impact on the field of earthquake science and related hazard assessment.

This special issue is a compilation of 43 papers on multidisciplinary research regarding this unique sequence, the relevant tectonics and associated phenomena with state-of-the-art techniques as well as traditional ones.

Many papers discuss source processes based on studies from the viewpoint of their own discipline, such as teleseismic seismograms, strong ground motion records and surface displacements detected by space geodesy. Yagi et al. (2016) reveal the temporal evolution of rupture using seismograms from a global network. In contrast, Asano and Iwata (2016), Kubo et al. (2016), Nozu and Nagasaka (2017) and Yoshida et al. (2017) discuss the detailed rupture process using strong ground motion records. Their modeled faults have significant differences among them in the number of faults and geometry, but similar characteristics in slip distribution and temporal evolution of rupture are derived. Nozu and Nagasaka (2017) assume a single planar fault, while Kubo et al. (2016) use a single, smoothly curved plane. Asano and Iwata (2016) assume two planar faults, and Yoshida et al. (2017) model four planar faults dipping in different directions. Uchide et al. (2016) also present a model of the rupture process of the mainshock and discuss its relationship with aftershocks. Sawazaki et al. (2016) exploit high-frequency records to derive temporal variations in energy release during the period spanning nearly the entire sequence. Fukuyama and Suzuki (2016) estimate Dc″, a proxy of critical slip-weakening displacement, based on a near-fault seismogram.

Since its launch in May 2014, the Advanced Land Observing Satellite 2 (ALOS-2) of the Japan Aerospace Exploration Agency has been providing us with invaluable information on deformation of the earth's surface. ALOS-2 made observations from many tracks with different line-of-sight directions. Using the data from ALOS-2, several groups present models of coseismic deformation on faults. Himematsu and Furuya (2016) exploit pixel offsets as well as phase changes to reveal deformation. Ozawa et al. (2016) present a model with four fault segments by fitting the observed interferograms of ALOS-2. Fukahata and Hashimoto (2016) invert interferograms of ALOS-2 ScanSAR images to simultaneously estimate the slip distribution and dip angle of two fault segments. Kobayashi (2017) exploit multiple aperture interferometry as well as conventional interferometry to reveal coseismic deformation due to foreshocks. Fujiwara et al. (2016) focus on detailed features of numerous surface ruptures recognized in ALOS-2 interferograms and present their qualitative mechanism in relation to faulting and geologic structures. As in the case of the strong-motion studies, there is a variety in the geometry and number of faults, reflecting the complexity of the rupture and observed deformations. This wide variety of fault models indicates a limitation in the ability of presently available techniques for the study of earthquake sources.

*Correspondence: hashimoto.manabu.7e@kyoto-u.ac.jp
[1] Disaster Prevention Research Institute, Kyoto University, Uji 611-0011, Kyoto, Japan
Full list of author information is available at the end of the article

Since the target region includes the active Aso volcano, which is located along the southern boundary of the Beppu-Shimabara graben zone, the relationship between rupture process and subsurface structure is considered important. Yagi et al. (2016) and Ozawa et al. (2016) discuss the effects of stress changes due to the rupture of the mainshock on the magma reservoir of Aso volcano. Aizawa et al. (2017) analyze broadband magnetotelluric data and reveal a three-dimensional distribution of resistivity to discuss its relationship to the seismicity. Kusumoto (2016) and Matsumoto N et al. (2016) analyze the gravity gradient tensor and examine its relationship to the geometry of source faults. Mochizuki and Mitsui (2016) discuss the relationship between heterogeneous structure and interseismic crustal deformation. Miyakawa et al. (2016) invert gravity data to reveal a low-density body beneath the Aso caldera and discuss its possible effect on the termination of rupture. Matsumoto S et al. (2016) perform a stress tensor inversion of fault plane solutions and seismic moment tensors in central Kyushu and reveal a zone of large inelastic strain.

As mentioned above, the high intensity of ground shaking is an important issue in this earthquake sequence. Zhang et al. (2016) simulate ground motion records assuming an attenuation structure and site effect and succeed in reproducing observed ground motion. Hata et al. (2016) also try to reproduce strong ground motion, especially near the Shinkansen (bullet train system in Japan) track, with special reference to site effects. Yamanaka et al. (2016) conduct dense observation of aftershocks in heavily damaged areas and find local amplification effects in Mashiki, Nishihara and Kumamoto, but not in Minami-Aso. Chimoto et al. (2016) conduct array analysis in Mashiki and Nishihara and obtain the S-wave velocity structure, which they consider controls site amplification. On the other hand, Kawase et al. (2017) make a detailed survey of damages and reanalyze strong-motion records in the Mashiki town, attributing severe structural damages to a strong westward velocity pulse, rather than to site effects. Tsuno et al. (2017) evaluate site amplification in Kumamoto based on dense observation of microtremor and conclude that site amplification is not enough to explain observed ground motion during the mainshock. Irikura et al. (2017) examine three rupture models of the mainshock of the Kumamoto earthquake sequence and verify the effectiveness of source scaling relations for crustal earthquakes. Suzuki et al. (2017) study attenuation on strong-motion records and present a feasible method for real-time forecasting of strong motions. Nagasaka and Nozu (2017) discuss the applicability of multiple point sources to strong ground motion prediction.

During the Kumamoto earthquake sequence, many surface ruptures appeared and their origin is controversial. Tajima et al. (2017) discuss the relationship between surface ruptures found within the Aso caldera and the distribution of volcanic edifices to derive a possible link between the source fault and volcanic vents. Sugito et al. (2016) reported a detailed distribution of surface ruptures associated with the foreshock, some of which also moved during the mainshock. Shirahama et al. (2016) also compile a distribution of surface ruptures and conclude that most of them are distributed along previously identified active faults. Toda et al. (2016) examine surface ruptures aligned parallel to each other near the Mashiki town and Nishihara village and present a model of slip partitioning. Goto et al. (2017) examine subtle geomorphic features of surface ruptures using a digital elevation model in the city of Kumamoto and discuss their possible relationship to the earthquake source faults.

Seismicity change prior to a large earthquake is always an issue. Nanjo et al. (2016) present results of analyses using four different methods and detected anomalous change in seismicity. Nanjo and Yoshida (2017) discuss changes in parameters that describe seismicity between the M6.5 foreshock and M7.3 mainshock. Zhuang et al. (2017) discuss the effects of newly developed replenishments of the missing data on estimated parameters of the epidemic-type aftershock sequence (ETAS) model. Yano and Matsubara (2017) relocate hypocenters and discuss detailed features of seismicity during different periods such as 2001–2012, between the foreshock and mainshock, and after the mainshock.

A moderate earthquake hit the Yufuin city, Oita prefecture, right after the occurrence of the M7.3 mainshock. This event is considered to have been triggered by the seismic waves that radiated from the source fault of the mainshock. This phenomenon attracted the interest of many researchers. Miyazawa (2016) carefully examines the timing of triggering of the earthquake in Yufuin, exploiting a full waveform simulation of the mainshock. Enescu et al. (2016) show the activation of seismicity in volcanic areas as far away as Hokkaido as well as in non-volcanic areas such as Noto peninsula. Yoshida (2016) re-estimates the magnitude of this triggered event using strong-motion records and GNSS data and concludes that the preliminary magnitude was underestimated. Uchide et al. (2016) also examine the magnitude of triggered events. Nakamura and Aoi (2017) estimate a focal mechanism and location of the triggered event in Yufuin.

Recent development of real-time monitoring for earthquake early warning is amazing. Applications of this newly deployed technique to the Kumamoto earthquake sequence are presented in this issue. Kawamoto et al. (2016) show the ability of the GNSS-based real-time analysis system (REGARD) deployed by the Geospatial Information Authority (GSI) to detect coseismic displacements and estimate size and location of the source fault. Kodera et al. (2016) examine the performance of the current seismic-based earthquake early warning system operated by the Japan Meteorological Agency (JMA) and indicate that two improved methods will be implemented in the near future.

This special issue is a compilation of preliminary works due to the limitation of available data and techniques, but gives deep insights into the generation process of this unique sequence of earthquakes. As the guest editors of this issue, we expect that these works will be a milestone for future studies of this earthquake sequence.

Authors' contributions
All authors of this article served as guest editors for this special issue. All authors read and approved the final manuscript.

Author details
[1] Disaster Prevention Research Institute, Kyoto University, Uji 611-0011, Kyoto, Japan. [2] Institute of Geophysics, SGEES, Victoria University of Wellington, Box 600, Wellington 6140, New Zealand. [3] Geological Survey of Japan, National Institute of Advanced Industrial Science and Technology, Tsukuba 305-0046, Ibaraki, Japan. [4] Faculty of Science and Engineering, Doshisha University, Kyotanabe 610-0394, Kyoto, Japan.

Acknowledgements
We express sincere thankfulness to the authors who contributed to this special issue, and reviewers who evaluated the contributions and gave helpful comments and suggestions.

Publisher's Note
Springer Nature remains neutral with regard to jurisdictional claims in published maps and institutional affiliations.

Received: 10 July 2017 Accepted: 10 July 2017
Published online: 24 July 2017

References
Aizawa K, Asaue H, Koike K, Takakura S, Utsugi M, Inoue H, Yoshimura R, Yamazaki K, Komatsu S, Uyeshima M, Koyama T, Kanda W, Shiotani T, Matsushima N, Hata M, Yoshinaga T (2017) Seismicity controlled by resistivity structure: the 2016 Kumamoto earthquakes, Kyushu Island, Japan. Earth Planets Space 69:4. doi:10.1186/s40623-016-0590-2
Asano K, Iwata T (2016) Source rupture processes of the foreshock and mainshock in the 2016 Kumamoto earthquake sequence estimated from the kinematic waveform inversion of strong motion data. Earth Planets Space 68:147. doi:10.1186/s40623-016-0519-9
Chimoto K, Yamanaka H, Tsuno S, Miyake H, Yamada N (2016) Estimation of shallow S-wave velocity structure using microtremor array exploration at temporary strong motion observation stations for aftershocks of the 2016 Kumamoto earthquake. Earth Planets Space 68:206. doi:10.1186/s40623-016-0581-3
Enescu B, Shimojo K, Opris A, Yagi Y (2016) Remote triggering of seismicity at Japanese volcanoes following the 2016 M7.3 Kumamoto earthquake. Earth Planets Space 68:165. doi:10.1186/s40623-016-0539-5
Fujiwara S, Yarai H, Kobayashi T, Morishita Y, Nakano T, Miyahara B, Nakai H, Miura Y, Ueshiba H, Kakiage Y, Une H (2016) Small-displacement linear surface ruptures of the 2016 Kumamoto earthquake sequence detected by ALOS-2 SAR interferometry. Earth Planets Space 68:160. doi:10.1186/s40623-016-0534-x
Fukahata Y, Hashimoto M (2016) Simultaneous estimation of the dip angles and slip distribution on the faults of the 2016 Kumamoto earthquake through a weak nonlinear inversion of InSAR data. Earth Planets Space 68:204. doi:10.1186/s40623-016-0580-4
Fukuyama E, Suzuki W (2016) Near-fault deformation and Dc″ during the 2016 Mw7.1 Kumamoto earthquake. Earth Planets Space 68:194. doi:10.1186/s40623-016-0570-6
Goto H, Tsutsumi H, Toda S, Kumahara Y (2017) Geomorphic features of surface ruptures associated with the 2016 Kumamoto earthquake in and around the downtown of Kumamoto City, and implications on triggered slip along active faults. Earth Planets Space 69:26. doi:10.1186/s40623-017-0603-9
Hata Y, Masaaki Yabe M, Kasai A, Matsuzaki H, Takahashi Y, Akiyama M (2016) Ground motion estimation for the elevated bridges of the Kyushu Shinkansen derailment caused by the foreshock of the 2016 Kumamoto earthquake based on the site-effect substitution method. Earth Planets Space 68:199. doi:10.1186/s40623-016-0573-3
Himematsu Y, Furuya M (2016) Fault source model for the 2016 Kumamoto earthquake sequence based on ALOS-2/PALSAR-2 pixel-offset data: evidence for dynamic slip partitioning. Earth Planets Space 68:169. doi:10.1186/s40623-016-0545-7 **(Erratum to this article has been published in Earth, Planets and Space 68:196)**
Irikura K, Miyakoshi K, Kamae K, Yoshida K, Somei K, Kurahashi S, Miyake H (2017) Applicability of source scaling relations for crustal earthquakes to estimation of the ground motions of the 2016 Kumamoto earthquake. Earth Planets Space 69:10. doi:10.1186/s40623-016-0586-y
Kawamoto S, Hiyama Y, Ohta Y, Nishimura T (2016) First result from the GEONET real-time analysis system (REGARD): the case of the 2016 Kumamoto earthquakes. Earth Planets Space 68:190. doi:10.1186/s40623-016-0564-4
Kawase H, Matsushima S, Nagashima F, Baoyintu Nakano K (2017) The cause of heavy damage concentration in downtown Mashiki inferred from observed data and field survey of the 2016 Kumamoto earthquake. Earth Planets Space 69:3. doi:10.1186/s40623-016-0591-1
Kobayashi T (2017) Earthquake rupture properties of the 2016 Kumamoto earthquake foreshocks (*M* j 6.5 and *M* j 6.4) revealed by conventional and multiple-aperture InSAR. Earth Planets Space 69:7. doi:10.1186/s40623-016-0594-y
Kodera Y, Saitou J, Hayashimoto N, Adachi S, Morimoto M, Nishimae Y, Hoshiba M (2016) Earthquake early warning for the 2016 Kumamoto earthquake: performance evaluation of the current system and the next-generation methods of the Japan Meteorological Agency. Earth Planets Space 68:202. doi:10.1186/s40623-016-0567-1
Kubo H, Suzuki W, Aoi S, Haruko Sekiguchi H (2016) Source rupture processes of the 2016 Kumamoto, Japan, earthquakes estimated from strong-motion waveforms. Earth Planets Space 68:161. doi:10.1186/s40623-016-0536-8
Kusumoto S (2016) Dip distribution of Oita-Kumamoto Tectonic Line located in central Kyushu, Japan, estimated by eigenvectors of gravity gradient tensor. Earth Planets Space 68:153. doi:10.1186/s40623-016-0529-7
Matsumoto N, Hiramatsu Y, Sawada A (2016) Continuity, segmentation and faulting type of active fault zones of the 02016 Kumamoto earthquake inferred from analyses of a gravity gradient tensor. Earth Planets Space 68:167. doi:10.1186/s40623-016-0541-y **(The Erratum to this article has been published in Earth, Planets and Space 69:47)**
Matsumoto S, Nishimura T, Ohkura T (2016) Inelastic strain rate in the seismogenic layer of Kyushu Island, Japan. Earth Planets Space 68:207. doi:10.1186/s40623-016-0584-0
Miyakawa A, Sumita T, Okubo Y, Okuwaki R, Otsubo M, Uesawa S, Yagi Y (2016) Volcanic magma reservoir imaged as a low-density body beneath Aso volcano that terminated the 2016 Kumamoto earthquake rupture. Earth Planets Space 68:208. doi:10.1186/s40623-016-0582-2
Miyazawa M (2016) An investigation into the remote triggering of the Oita earthquake by the 2016 Mw 7.0 Kumamoto earthquake using full wavefield simulation. Earth Planets Space 68:205. doi:10.1186/s40623-016-0585-z
Mochizuki K, Mitsui Y (2016) Crustal deformation model of the Beppu-Shimabara graben area, central Kyushu, Japan, based on inversion of three-component GNSS data in 2000–2010. Earth Planets Space 68:177. doi:10.1186/s40623-016-0550-x

Nagasaka Y, Nozu A (2017) Strong ground motion simulation of the 2016 Kumamoto earthquake of April 16 using multiple point sources. Earth Planets Space 69:25. doi:10.1186/s40623-017-0612-8
Nakamura T, Aoi S (2017) Source location and mechanism analysis of an earthquake triggered by the 2016 Kumamoto, southwestern Japan, earthquake. Earth Planets Space 69:6. doi:10.1186/s40623-016-0588-9
Nanjo KZ, Yoshida A (2017) Anomalous decrease in relatively large shocks and increase in the *p* and *b* values preceding the April 16, 2016, *M*7.3 earthquake in Kumamoto, Japan. Earth Planets Space 69:13. doi:10.1186/s40623-017-0598-2
Nanjo KZ, Izutsu J, Orihara Y, Furuse N, Togo S, Nitta H, Okada T, Tanaka R, Kamogawa M, Nagao T (2016) Seismicity prior to the 2016 Kumamoto earthquakes. Earth Planets Space 68:187. doi:10.1186/s40623-016-0558-2
Nozu A, Nagasaka Y (2017) Rupture process of the main shock of the 2016 Kumamoto earthquake with special reference to damaging ground motions: waveform inversion with empirical Green's functions. Earth Planets Space 69:22. doi:10.1186/s40623-017-0609-3
Ozawa T, Fujita E, Ueda H (2016) Crustal deformation associated with the 2016 Kumamoto Earthquake and its effect on the magma system of Aso volcano. Earth Planets Space 68:186. doi:10.1186/s40623-016-0563-5
Sawazaki K, Nakahara H, Shiomi K (2016) Preliminary estimation of high-frequency (4–20 Hz) energy released from the 2016 Kumamoto, Japan, earthquake sequence. Earth Planets Space 68:183. doi:10.1186/s40623-016-0557-3
Shirahama Y, Yoshimi M, Awata Y, Maruyama T, Azuma T, Miyashita Y, Mori H, Imanishi K, Takeda N, Ochi T, Otsubo M, Asahina D, Miyakawa A (2016) Characteristics of the surface ruptures associated with the 2016 Kumamoto earthquake sequence, central Kyushu, Japan. Earth Planets Space 68:191. doi:10.1186/s40623-016-0559-1
Sugito N, Goto H, Kumahara Y, Tsutsumi H, Nakata T, Kagohara K, Matsuta N, Yoshida H (2016) Surface fault ruptures associated with the 14 April foreshock (Mj 6.5) of the 2016 Kumamoto earthquake sequence, southwest Japan. Earth Planets Space 68:170. doi:10.1186/s40623-016-0547-5
Suzuki W, Aoi S, Kunugi T, Kubo H, Morikawa N, Nakamura H, Kimura T, Fujiwara H (2017) Strong motions observed by K-NET and KiK-net during the 2016 Kumamoto earthquake sequence. Earth Planets Space 69:19. doi:10.1186/s40623-017-0604-8
Tajima Y, Hasenaka T, Torii M (2017) Effects of the 2016 Kumamoto earthquakes on the Aso volcanic edifice. Earth Planets Space 69:63. doi:10.1186/s40623-017-0646-y
Toda S, Kaneda H, Okada S, Ishimura D, Mildon ZK (2016) Slip-partitioned surface ruptures for the Mw 7.0 16 April 2016 Kumamoto, Japan, earthquake. Earth Planets Space 68:188. doi:10.1186/s40623-016-0560-8
Tsuno S, Korenaga M, Okamoto K, Yamanaka H, Chimoto K, Matsushima T (2017) Local site effects in Kumamoto City revealed by the 2016 Kumamoto earthquake. Earth Planets Space 69:37. doi:10.1186/s40623-017-0622-6
Uchide T, Horikawa H, Nakai M, Matsushita R, Shigematsu N, Ando R, Imanishi K (2016) The 2016 Kumamoto–Oita earthquake sequence: aftershock seismicity gap and dynamic triggering in volcanic areas. Earth Planets Space 68:180. doi:10.1186/s40623-016-0556-4
Yagi Y, Okuwaki R, Enescu B, Kasahara A, Miyakawa A, Otsubo M (2016) Rupture process of the 2016 Kumamoto earthquake in relation to the thermal structure around Aso volcano. Earth Planets Space 68:118. doi:10.1186/s40623-016-0492-3
Yamanaka H, Chimoto K, Miyake H, Tsuno S, Yamada N (2016) Observation of earthquake ground motion due to aftershocks of the 2016 Kumamoto earthquake in damaged areas. Earth Planets Space 68:197. doi:10.1186/s40623-016-0574-2
Yano TE, Matsubara M (2017) Effect of newly refined hypocenter locations on the seismic activity recorded during the 2016 Kumamoto Earthquake sequence. Earth Planets Space 69:74. doi:10.1186/s40623-017-0656-9
Yoshida S (2016) Earthquakes in Oita triggered by the 2016 *M*7.3 Kumamoto earthquake. Earth Planets Space 68:176. doi:10.1186/s40623-016-0552-8
Yoshida K, Miyakoshi K, Somei K, Irikura K (2017) Source process of the 2016 Kumamoto earthquake (Mj7.3) inferred from kinematic inversion of strong-motion records. Earth Planets Space 69:64. doi:10.1186/s40623-017-0649-8
Zhang L, Chen G, Wu Y (2016) Jiang H (2016) Stochastic ground-motion simulations for the 2016 Kumamoto, Japan, earthquake. Earth Planets Space 68:184. doi:10.1186/s40623-016-0565-3
Zhuang J, Ogata Y, Wang T (2017) Data completeness of the Kumamoto earthquake sequence in the JMA catalog and its influence on the estimation of the ETAS parameters. Earth Planets Space 69:36. doi:10.1186/s40623-017-0614-6

FRONTIER LETTER Open Access

Rupture process of the 2016 Kumamoto earthquake in relation to the thermal structure around Aso volcano

Yuji Yagi*, Ryo Okuwaki, Bogdan Enescu, Amato Kasahara, Ayumu Miyakawa and Makoto Otsubo

Earth, Planets and Space 2016, **68**:118 doi:10.1186/s40623-016-0492-3
Received: 5 May 2016, Accepted: 15 June 2016, Published: 14 July 2016

Abstract

We constructed the rupture process model for the 2016 Kumamoto, Japan, earthquake from broadband teleseismic body waveforms (P-waves) by using a novel waveform inversion method that takes into account the uncertainty of Green's function. The estimated source parameters are: seismic moment = 5.1×10^{19} Nm (Mw = 7.1), fault length = 40 km, and fault width = 15 km. The mainshock rupture mainly propagated northeastward from the epicenter, for about 30 km, along an active strike-slip fault. The rupture propagation of the mainshock decelerated and terminated near the southwest side of the Aso volcano; the aftershock activity was low around the northeastern edge of the major slip area. Our results suggest that the rupture process of the mainshock and the distribution of aftershocks were influenced by the high-temperature area around the magma chamber of Mt. Aso.

Keywords: 2016 Kumamoto earthquake, Rupture process, Foreshocks and aftershocks, Mt. Aso, Magma chamber

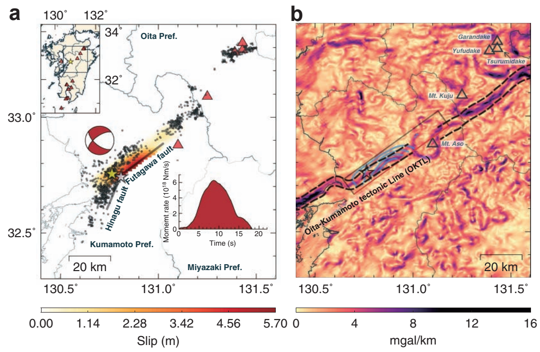

Figure 1

*Corresponding author: Yuji Yagi, yagi-y@geol.tsukuba.ac.jp

FRONTIER LETTER Open Access

Source rupture processes of the foreshock and mainshock in the 2016 Kumamoto earthquake sequence estimated from the kinematic waveform inversion of strong motion data

Kimiyuki Asano* and Tomotaka Iwata

Earth, Planets and Space 2016, **68**:147 doi:10.1186/s40623-016-0519-9
Received: 17 May 2016, Accepted: 29 July 2016, Published: 31 August 2016

Abstract

The 2016 Kumamoto earthquake sequence started with an M_{JMA} 6.5 foreshock occurring along the northern part of the Hinagu fault, central Kyushu, Japan, and the M_{JMA} 7.3 mainshock occurred just 28 h after the foreshock. We analyzed the source rupture processes of the foreshock and mainshock by using the kinematic waveform inversion technique on strong motion data. The foreshock was characterized by right-lateral strike-slip occurring on a nearly vertical fault plane along the northern part of the Hinagu fault, and it had two large-slip areas: one near the hypocenter and another at a shallow depth. The rupture of the mainshock started from the deep portion of a northwest-dipping fault plane along the northern part of the Hinagu fault, then continued to transfer to the Futagawa fault. Most of the significant slip occurred on the Futagawa fault, and the shallow portion of the Hinagu fault also had a relatively large slip. The slip amount on the shallowest subfaults along the Futagawa fault was approximately 1–4 m, which is consistent with the emergence of surface breaks associated with this earthquake. Right-lateral strike-slip dominated on the fault segment along the Hinagu fault, but normal-slip components were estimated to make a significant contribution on the fault segment along the Futagawa fault. The large fault-parallel displacements recorded at two near-fault strong motion stations coincided with the spatiotemporal pattern of the fault slip history during the mainshock. The spatial relationship between the rupture areas of the foreshock and mainshock implies a complex fault structure in this region.

Keywords: 2016 Kumamoto earthquake, Source rupture process, Kinematic source inversion, Strong motion data, Futagawa and Hinagu faults

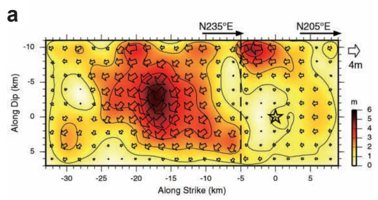

Figure 5

*Corresponding author: Kimiyuki Asano, k-asano@egmdpri01.dpri.kyoto-u.ac.jp

FRONTIER LETTER **Open Access**

Slip-partitioned surface ruptures for the Mw 7.0 16 April 2016 Kumamoto, Japan, earthquake

Shinji Toda*, Heitaro Kaneda, Shinsuke Okada, Daisuke Ishimura and Zoë K. Mildon

Earth, Planets and Space 2016, **68**:188 doi:10.1186/s40623-016-0560-8
Received: 15 July 2016, Accepted: 29 October 2016, Published: 22 November 2016

Abstract

An ENE-trending ~30-km-long surface rupture emerged during the Mw = 7.0 16 April 2016 Kumamoto earthquake along the previously mapped Futagawa and northern Hinagu faults. This included a previously unknown 5-km-long fault within the Aso Caldera, central Kyushu. The rupture zone is mostly composed of right-lateral slip sections, with a maximum of 2-m coseismic slip. One of the noteworthy features we observed in the field are ~10-km-long segmented normal fault scarps, dipping to the northwest, along the previously mapped Idenokuchi fault, 1.2–2.0 km south of and subparallel to the Futagawa fault. The maximum amount of coseismic throw on the Idenokuchi fault is ~2 m, which is nearly equivalent to the maximum slip on the strike-slip rupture. The locations and slip motions of the 2016 rupture are also manifested as interferogram fringe offsets in InSAR images. Together with geodetic and seismic inversions of subsurface fault slip, we present a schematic structural model where oblique motion occurred on a northwest-dipping subsurface fault and the slip is partitioned at the surface into strike-slip and normal fault scarps. Our simple dislocation model demonstrates that this bifurcation into pure strike-slip and normal faults likely occurs for optimally oriented failure near the surface. The Kumamoto case, with detailed geological observations and geophysical models, would be the second significant slip-partitioned earthquake around the globe. It provides an important insight into scale- and depth-dependent stress heterogeneity and an implication to a proper estimate of seismic hazard in complex and broad multiple fault strands.

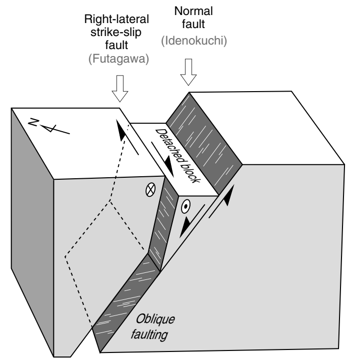

Figure 7

Keywords: 2016 Kumamoto earthquake, Surface rupture, Slip partitioning, Active fault

*Corresponding author: Shinji Toda, toda@irides.tohoku.ac.jp

FULL PAPER **Open Access**

Small-displacement linear surface ruptures of the 2016 Kumamoto earthquake sequence detected by ALOS-2 SAR interferometry

Satoshi Fujiwara*, Hiroshi Yarai, Tomokazu Kobayashi, Yu Morishita, Takayuki Nakano, Basara Miyahara, Hiroyuki Nakai, Yuji Miura, Haruka Ueshiba, Yasuaki Kakiage and Hiroshi Une

Earth, Planets and Space 2016, **68**:160 doi:10.1186/s40623-016-0534-x
Received: 29 June 2016, Accepted: 6 September 2016, Published: 26 September 2016

Abstract

We constructed and analyzed the ground surface displacement associated with the 2016 Kumamoto earthquake sequence using satellite radar interferometry images of the Advanced Land Observing Satellite 2. The radar interferogram generally shows elastic deformation caused by the main earthquakes, but many other linear discontinuities showing displacement are also found. Approximately 230 lineaments are identified, some of which coincide with the positions of known active faults, such as the main earthquake faults belonging to the Futagawa and Hinagu fault zones and other minor faults; however, there are much fewer known active faults than lineaments. In each area, the lineaments have a similar direction and displacement to each other; therefore, they can be divided into several groups based on location and major features. Since the direction of the lineaments coincides with that of known active faults or their conjugate faults, the cause of the lineaments must be related to the tectonic stress field of this region. The lineaments are classified into the following two categories: (1) main earthquake faults and their branched subfaults and (2) secondary faults that are not directly related to the main earthquake but whose slip was probably triggered by the main earthquake or aftershocks.

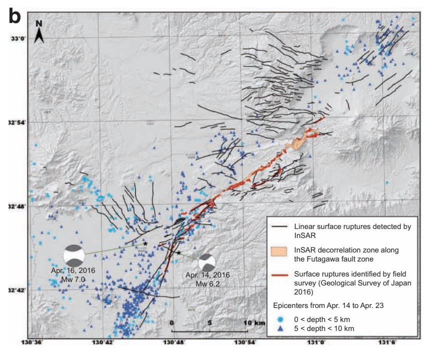

Figure 2

Keywords: 2016 Kumamoto earthquake sequence, ALOS-2, SAR interferometry, Linear surface rupture

*Corresponding author: Satoshi Fujiwara, fujiwara-s2vq@mlit.go.jp

FULL PAPER **Open Access**

Remote triggering of seismicity at Japanese volcanoes following the 2016 M7.3 Kumamoto earthquake

Bogdan Enescu*, Kengo Shimojo, Anca Opris and Yuji Yagi

Earth, Planets and Space 2016, **68**:165 doi:10.1186/s40623-016-0539-5
Received: 7 July 2016, Accepted: 27 September 2016, Published: 20 October 2016

Abstract

The M_{JMA}7.3 Kumamoto earthquake occurred on April 16, 2016, in the western part of Kyushu, at a depth of 12 km, on an active strike-slip fault. Here, we report on a relatively widespread activation of small remote earthquakes, which occurred as far as Hokkaido, detected by analyzing the continuous waveform data recorded at seismic stations all over Japan. Such relatively widespread remote seismicity activation, following a large inland earthquake, has not been reported before for Japan. Our analysis demonstrates that the remote events were triggered dynamically, by the passage of the surface waves from the Kumamoto earthquake. Most of the remotely triggered events in the Tohoku and Hokkaido regions, as well as close to Izu Peninsula, occur at or close to volcanoes, which suggests that the excitation of crustal fluids, by the passage of Rayleigh waves, played an important triggering role. Nevertheless, remote activation in other regions, like Noto Peninsula, occurred away from volcanoes. The relatively large-amplitude Love waves, enhanced by a source directivity effect during the Kumamoto earthquake, may have triggered seismicity on local active faults. The dynamic stresses in the areas where remote activation has been observed range from several kPa to tens of kPa, the thresholds being lower than in previous dynamic triggering cases for Japan; this might relate to a change in the crustal conditions following the 2011 M9.0 Tohoku-oki earthquake, in particular at volcanoes in NE Japan.

Keywords: Kumamoto earthquake, Remote triggering, Volcanoes, Active faults, Dynamic stresses

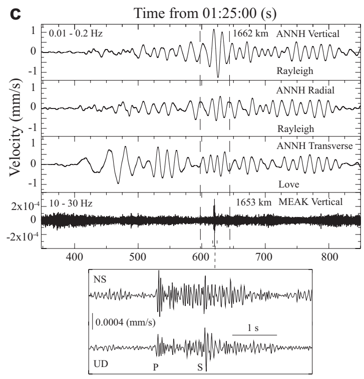

Figure 3

*Corresponding author: Bogdan Enescu, benescu@kugi.kyoto-u.ac.jp

FULL PAPER **Open Access**

Preliminary estimation of high-frequency (4–20 Hz) energy released from the 2016 Kumamoto, Japan, earthquake sequence

Kaoru Sawazaki*, Hisashi Nakahara and Katsuhiko Shiomi

Earth, Planets and Space 2016, **68**:183 doi:10.1186/s40623-016-0557-3
Received: 25 July 2016, Accepted: 29 October 2016, Published: 23 November 2016

Abstract

We estimate high-frequency (4–20 Hz) energy release due to the 2016 Kumamoto, Japan, earthquake sequence, within a time period from April 14 to 26 through envelope inversion analysis applied to the Hi-net continuous seismograms. We especially focus on energy releases after each of the April 14 M_{JMA}6.5 and the April 16 M_{JMA}7.3 earthquakes. The cumulative energy release from aftershocks of the April 14 event reaches 60% of that from the April 14 event itself by the lapse time of 27 h (pre-April 16 period). On the other hand, the cumulative energy release from aftershocks of the April 16 event reaches only 11 and 13% of that from the April 16 event itself by the lapse times of 27 h and 10 days (post-April 16 period), respectively. This discrepancy in the normalized cumulative energy release (NCER) indicates that the April 14 event was followed by much larger relative aftershock productivity than the April 16 event. Thus, NCER would provide information that reflects relative aftershock productivity and ongoing seismicity pattern after a large earthquake. We also find that the temporal decay of the energy release rate obeys the power law. The exponent p_E of the power-law decay is estimated to be 1.7–2.1, which is much larger than the typical p value of the Omori–Utsu law: slightly larger than 1. We propose a simple relationship given by $p_E = \beta p/b$, where p value, b value of the Gutenberg–Richter law, and β value of the magnitude–energy release relationship are combined.

Keywords: 2016 Kumamoto earthquake sequence, Aftershocks, High-frequency energy release, Normalized cumulative energy release

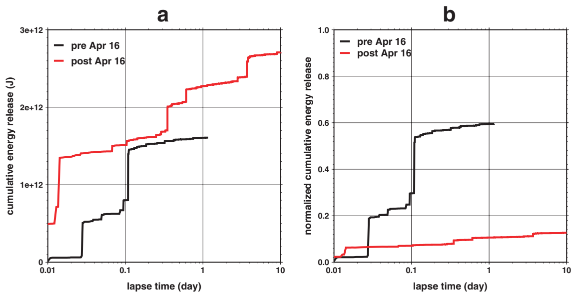

Figure 9

*Corresponding author: Kaoru Sawazaki, sawa@bosai.go.jp

FULL PAPER **Open Access**

Stochastic ground-motion simulations for the 2016 Kumamoto, Japan, earthquake

Long Zhang*, Guangqi Chen, Yanqiang Wu and Han Jiang

Earth, Planets and Space 2016, **68**:184 doi:10.1186/s40623-016-0565-3
Received: 16 June 2016, Accepted: 5 November 2016, Published: 18 November 2016

Abstract

On April 15, 2016, Kumamoto, Japan, was struck by a large earthquake sequence, leading to severe casualty and building damage. The stochastic finite-fault method based on a dynamic corner frequency has been applied to perform ground-motion simulations for the 2016 Kumamoto earthquake. There are 53 high-quality KiK-net stations available in the Kyushu region, and we employed records from all stations to determine region-specific source, path and site parameters. The calculated *S*-wave attenuation for the Kyushu region beneath the volcanic and non-volcanic areas can be expressed in the form of $Q_s = (85.5 \pm 1.5)f^{0.68\pm0.01}$ and $Q_s = (120 \pm 5)f^{0.64\pm0.05}$, respectively. The effects of lateral *S*-wave velocity and attenuation heterogeneities on the ground-motion simulations were investigated. Site amplifications were estimated using the corrected cross-spectral ratios technique. Zero-distance kappa filter was obtained to be the value of 0.0514 ± 0.0055 s, using the spectral decay method. The stress drop of the mainshock based on the USGS slip model was estimated optimally to have a value of 64 bars. Our finite-fault model with optimized parameters was validated through the good agreement of observations and simulations at all stations. The attenuation characteristics of the simulated peak ground accelerations were also successfully captured by the ground-motion prediction equations. Finally, the ground motions at two destructively damaged regions, Kumamoto Castle and Minami Aso village, were simulated. We conclude that the stochastic finite-fault method with well-determined parameters can reproduce the ground-motion characteristics of the 2016 Kumamoto earthquake in both the time and frequency domains. This work is necessary for seismic hazard assessment and mitigation.

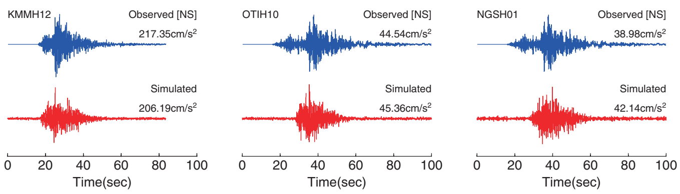

Figure 8

Keywords: Ground-motion simulations, Stochastic finite-fault method, 2016 Kumamoto earthquake

*Corresponding author: Long Zhang, zhanglong98524@163.com

FULL PAPER **Open Access**

Crustal deformation associated with the 2016 Kumamoto Earthquake and its effect on the magma system of Aso volcano

Taku Ozawa*, Eisuke Fujita and Hideki Ueda

Earth, Planets and Space 2016, **68**:186 doi:10.1186/s40623-016-0563-5
Received: 22 June 2016, Accepted: 5 November 2016, Published: 22 November 2016

Abstract

An M_{JMA}6.5 earthquake (foreshock) and M_{JMA}7.3 earthquake (mainshock) struck Kumamoto Prefecture on April 14, 2016, and April 16, 2016. To evaluate the effect of crustal deformation due to the earthquake on the Aso magma system, we detected crustal deformation using InSAR and GNSS. From InSAR analysis, we detected large crustal deformations along the Hinagu Fault, the Futagawa Fault, and the northeast extension of the latter fault. It extended to more than 50 km, and the maximum slant-range change exceeded 1 m. Although the obtained crustal deformation was approximately explained by the right-lateral strike-slip on the fault, its details could not be explained by such simple faulting. Additionally, we found complex surface deformation west of the Aso caldera rim, suggesting that shallow fault slips occurred in many known and unknown faults associated with the earthquake. Most of the crustal deformation could be reasonably explained by four rectangle faults located along the Futagawa Fault, in the northeast extension of the Futagawa Fault, alongside the Hinagu Fault, and in the eastern part of the Futagawa Fault. The first three of faults have high dip angles and right-lateral slip. The other was a fault with a low dip angle that branched from the shallow depth of the fault along the Futagawa Fault. The normal-dip right-lateral slip was estimated for this segment. Based on the estimated fault model, we calculated the displacement and stress field around the Aso volcano by the finite-element method (FEM) to evaluate the effects on the Aso magma system. In this calculation, we assumed a spherical soft medium located at a 6-km depth beneath the area south of the Kusasenri region as the magma system and considered only static effects. The result shows complex distributions of displacements and stresses, but we can notice the following significant points. (1) The spherical magma system deformed to an ellipsoid, and the total volume was slightly increased, less than 1%. (2) The differential stress around the upper portion of the magma system was as large as 3.5 MPa. This is strong enough to open pre-existing cracks and can cause the migration of magma.

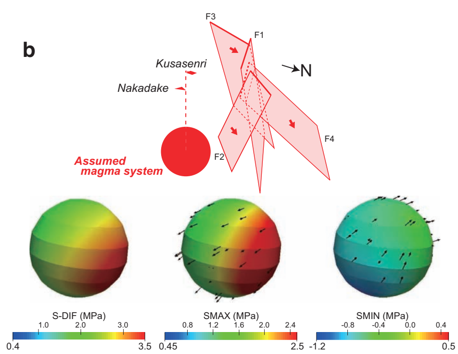

Figure 9

Keywords: Kumamoto Earthquake, Aso volcano, crustal deformation, InSAR, GNSS, fault model, effect on magma system

*Corresponding author: Taku Ozawa, taku@bosai.go.jp

FULL PAPER Open Access

Seismicity prior to the 2016 Kumamoto earthquakes

Kazuyoshi Z. Nanjo, Jun Izutsu, Yoshiaki Orihara, Nobuhiro Furuse, Shoho Togo, Hidetoshi Nitta, Tomohiro Okada, Rika Tanaka, Masashi Kamogawa and Toshiyasu Nagao*

Earth, Planets and Space 2016, **68**:187 doi:10.1186/s40623-016-0558-2
Received: 1 August 2016, Accepted: 29 October 2016, Published: 22 November 2016

Abstract

We report precursory seismic patterns prior to the 2016 Kumamoto earthquakes, as measured by four different methods based on changes in seismicity that can be used for earthquake forecasting: the *b*-value method, two methods of seismic quiescence evaluation, and an analysis of seismicity density in space and time. The spatial extent of precursory patterns differs from one method to the other and ranges from local scales (typically, asperity size) to regional scales (e.g., 2° × 3° around the source zone). The earthquakes were preceded by periods of pronounced anomalies, which lasted in yearly scales (1.5 years), or longer (>3 years). We demonstrate that a combination of multiple methods detected different signals prior to the Kumamoto earthquakes. This indicates great potential to reduce the hazard at possible future sites of earthquakes relative to long-term seismic hazard assessment. We also found that the seismic quiescence in a regional-scale area, detected by using the two methods of seismic quiescence evaluation, was a common precursor to the 2016 Kumamoto earthquakes and 2015 Off Satsuma Peninsula earthquake. The result allows us to interpret both events as the onset that occurred at a section along the tectonic line from the Okinawa Trough through the Beppu–Shimabara graben.

Keywords: Crustal deformation, Earthquake, Physical property of rocks, Time-series analysis, Probabilistic forecasting, Computational seismology, Statistical seismology, 2016 Kumamoto earthquakes, Critical phenomenon

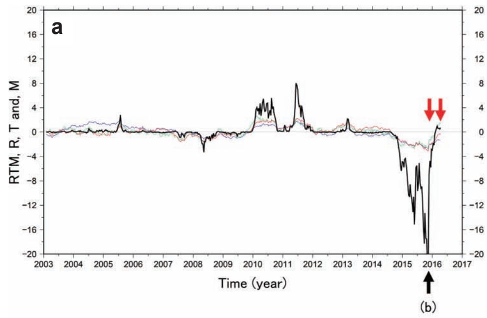

Figure 2

*Corresponding author: Toshiyasu Nagao, nagao@scc.u-tokai.ac.jp

FULL PAPER Open Access

First result from the GEONET real-time analysis system (REGARD): the case of the 2016 Kumamoto earthquakes

Satoshi Kawamoto*, Yohei Hiyama, Yusaku Ohta and Takuya Nishimura

Earth, Planets and Space 2016, **68**:190 doi:10.1186/s40623-016-0564-4
Received: 11 July 2016, Accepted: 5 November 2016, Published: 22 November 2016

Abstract

We present the initial results of rapid fault estimations for the 2016 Kumamoto earthquake on April 16 (M_j 7.3), and coseismic displacements caused by the two large foreshocks that occurred on April 14 (M_j 6.5) and April 15 (M_j 6.4) from the GEONET real-time analysis system (REGARD), which is based on a Global Navigation Satellite System (GNSS) kinematic positioning technique. The real-time finite-fault estimate (M_w 6.85) was obtained within 1 min and converged to M_w 6.96 within 5 min of the origin time of the mainshock (M_j 7.3). The finite-fault estimate shows right-lateral strike-slip fault along the Futagawa fault segment, which is consistent with the finite-fault model inferred from post-processed GNSS and InSAR analysis. Furthermore, significant coseismic displacements were observed due to the April 14 and April 15 foreshocks at nearby sites, though these earthquakes were smaller than the pre-assigned system threshold. Our results also demonstrate the potential for the GNSS-based earthquake early warning system for inland earthquakes.

Keywords: GNSS real-time positioning, Real-time magnitude estimation, Rapid source extent estimation, The 2016 Kumamoto earthquakes

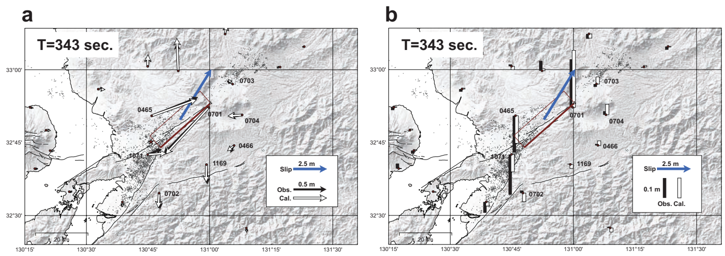

Figure 4

*Corresponding author: Satoshi Kawamoto, kawamoto-s96tf@mlit.go.jp

FULL PAPER **Open Access**

Earthquake early warning for the 2016 Kumamoto earthquake: performance evaluation of the current system and the next-generation methods of the Japan Meteorological Agency

Yuki Kodera*, Jun Saitou, Naoki Hayashimoto, Shimpei Adachi, Masahiko Morimoto, Yuji Nishimae and Mitsuyuki Hoshiba

Earth, Planets and Space 2016, **68**:202 doi:10.1186/s40623-016-0567-1
Received: 13 July 2016, Accepted: 15 November 2016, Published: 1 December 2016

Abstract

The 2016 Kumamoto earthquake (Kumamoto earthquake sequence) is an extremely high-seismicity event that has been occurring across Kumamoto and Oita Prefectures in Japan since April 14, 2016 (JST). The earthquake early warning system of the Japan Meteorological Agency (JMA) issued warnings for 19 events in the Kumamoto earthquake sequence from April 14 to 19, under some of the heaviest loading conditions since the system began operating in 2007. We analyzed the system performance for cases where a warning was issued and/or strong motion was actually observed. The results indicated that the system exhibited remarkable performance, especially for the most destructive earthquakes in the Kumamoto earthquake sequence. In addition, the system did not miss or seriously under-predict strong motion of any large earthquake from April 14 to 30. However, in four cases, the system issued over-predicted warnings due to the simultaneous occurrence of small earthquakes within a short distance, which implies a fundamental obstacle in trigger-data classifications based solely on arrival time. We also performed simulations using the integrated particle filter (IPF) and propagation of local undamped motion (PLUM) methods, which JMA plans to implement to address over-prediction for multiple simultaneous earthquakes and under-prediction for massive earthquakes with large rupture zones. The simulation results of the IPF method indicated that the IPF method is highly effective at minimizing over-prediction even for multiple simultaneous earthquakes within a short distance, since it adopts a trigger-data classification using velocity amplitude and hypocenter determinations using not-yet-arrived data. The simulation results of the PLUM method demonstrated that the PLUM method is capable of issuing warnings for destructive inland earthquakes more rapidly than the current system owing to the use of additional seismometers that can only be incorporated by this method.

Keywords: Earthquake early warning, 2016 Kumamoto earthquake, Integrated particle filter method, Propagation of local undamped motion method

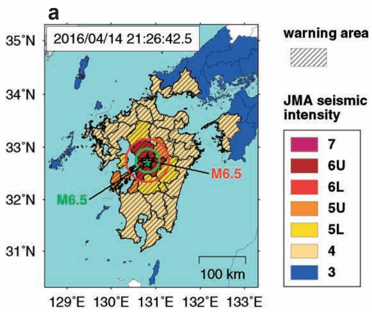

Figure 4

*Corresponding author: Yuki Kodera, kodera@mri-jma.go.jp

FULL PAPER **Open Access**

Simultaneous estimation of the dip angles and slip distribution on the faults of the 2016 Kumamoto earthquake through a weak nonlinear inversion of InSAR data

Yukitoshi Fukahata* and Manabu Hashimoto

Earth, Planets and Space 2016, **68**:204 doi:10.1186/s40623-016-0580-4
Received: 1 August 2016, Accepted: 29 November 2016, Published: 19 December 2016

Abstract

At the 2016 Kumamoto earthquake, surface ruptures were observed not only along the Futagawa fault, where main ruptures occurred, but also along the Hinagu fault. To estimate the slip distribution on these faults, we extend a method of nonlinear inversion analysis (Fukahata and Wright in Geophys J Int 173:353-364, 2008) to a two-fault system. With the method of Fukahata and Wright (2008), we can simultaneously determine the optimal dip angle of a fault and the slip distribution on it, based on Akaike's Bayesian information criterion by regarding the dip angle as an hyperparameter. By inverting the InSAR data with the developed method, we obtain the dip angles of the Futagawa and Hinagu faults as 61° ± 6° and 74° ± 12°, respectively. The slip on the Futagawa fault is mainly strike slip. The largest slip on it is over 5 m around the center of the model fault (130.9° in longitude) with a significant normal slip component. The slip on the Futagawa fault quickly decreases to zero beyond the intersection with the Hinagu fault. On the other hand, the slip has a local peak just inside Aso caldera, which would be a cause of severe damage in this area. A relatively larger reverse fault slip component on a deeper part around the intersection with Aso caldera suggests that something complicated happened there. The slip on the Hinagu fault is almost a pure strike slip with a peak of about 2.4 m. The developed method is useful in clarifying the slip distribution, when a complicated rupture like the Kumamoto earthquake happens in a remote area.

Keywords: The 2016 Kumamoto earthquake, Inversion analysis, InSAR, ABIC, Weak nonlinear inversion

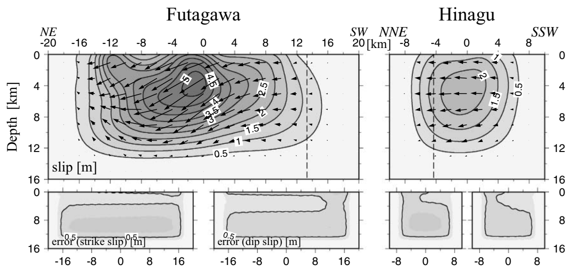

Figure 4

*Corresponding author: Yukitoshi Fukahata, fukahata@rcep.dpri.kyoto-u.ac.jp

FULL PAPER Open Access

Applicability of source scaling relations for crustal earthquakes to estimation of the ground motions of the 2016 Kumamoto earthquake

Kojiro Irikura*, Ken Miyakoshi, Katsuhiro Kamae, Kunikazu Yoshida, Kazuhiro Somei, Susumu Kurahashi and Hiroe Miyake

Earth, Planets and Space 2017, **69**:10 doi:10.1186/s40623-016-0586-y
Received: 11 August 2016, Accepted: 7 December 2016, Published: 3 January 2017

Abstract

A two-stage scaling relationship of the source parameters for crustal earthquakes in Japan has previously been constructed, in which source parameters obtained from the results of waveform inversion of strong motion data are combined with parameters estimated based on geological and geomorphological surveys. A three-stage scaling relationship was subsequently developed to extend scaling to crustal earthquakes with magnitudes greater than M_w 7.4. The effectiveness of these scaling relationships was then examined based on the results of waveform inversion of 18 recent crustal earthquakes (M_w5.4–6.9) that occurred in Japan since the 1995 Hyogo-ken Nanbu earthquake. The 2016 Kumamoto earthquake, with M_w 7.0, was one of the largest earthquakes to occur since dense and accurate strong motion observation networks, such as K-NET and KiK-net, were deployed after the 1995 Hyogo-ken Nanbu earthquake. We examined the applicability of the scaling relationships of the source parameters of crustal earthquakes in Japan to the 2016 Kumamoto earthquake. The rupture area and asperity area were determined based on slip distributions obtained from waveform inversion of the 2016 Kumamoto earthquake observations. We found that the relationship between the rupture area and the seismic moment for the 2016 Kumamoto earthquake follows the second-stage scaling within one standard deviation ($\sigma = 0.14$). The ratio of the asperity area to the rupture area for the 2016 Kumamoto earthquake is nearly the same as ratios previously obtained for crustal earthquakes. Furthermore, we simulated the ground motions of this earthquake using a characterized source model consisting of strong motion generation areas (SMGAs) based on the empirical Green's function (EGF) method. The locations and areas of the SMGAs were determined through comparison between the synthetic ground motions and observed motions. The sizes of the SMGAs were nearly coincident with the asperities with large slip. The synthetic ground motions obtained using the EGF method agree well with the observed motions in terms of acceleration, velocity, and displacement within the frequency range of 0.3–10 Hz. These findings indicate that the 2016 Kumamoto earthquake is a standard event that follows the scaling relationship of crustal earthquakes in Japan.

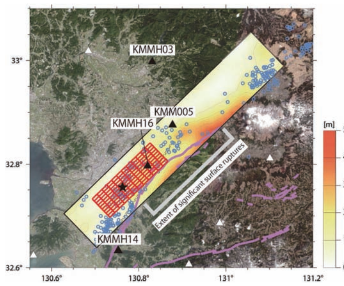

Figure 9

Keywords: Scaling relationship, Crustal earthquake, Source model, Strong ground motion prediction, Characterized source model, Strong motion generation area

*Corresponding author: Kojiro Irikura, irikura@geor.or.jp

FULL PAPER Open Access

Anomalous decrease in relatively large shocks and increase in the *p* and *b* values preceding the April 16, 2016, *M*7.3 earthquake in Kumamoto, Japan

K. Z. Nanjo* and A. Yoshida

Earth, Planets and Space 2017, **69**:13 /doi:10.1186/s40623-017-0598-2
Received: 1 August 2016, Accepted: 6 January 2017, Published: 14 January 2017

Abstract

The 2016 Kumamoto earthquakes in Kyushu, Japan, started with a magnitude (M) 6.5 quake on April 14 on the Hinagu fault zone (FZ), followed by active seismicity including an M6.4 quake. Eventually, an M7.3 quake occurred on April 16 on the Futagawa FZ. We investigated if any sign indicative of the M7.3 quake could be found in the space–time changes in seismicity after the M6.5 quake. As a quality control, we determined in advance the threshold magnitude, above which all earthquakes are completely recorded. We then showed that the occurrence rate of relatively large ($M \geq 3$) earthquakes significantly decreased 1 day before the M7.3 quake. Significance of this decrease was evaluated by one standard deviation of sampled changes in the rate of occurrence. We next confirmed that seismicity with $M \geq 3$ was well modeled by the Omori–Utsu law with $p \sim 1.5 \pm 0.3$, which indicates that the temporal decay of seismicity was significantly faster than a typical decay with $p = 1$. The larger p value was obtained when we used data of the longer time period in the analysis. This significance was confirmed by a bootstrapping approach. Our detailed analysis shows that the large p value was caused by the rapid decay of the seismicity in the northern area around the Futagawa FZ. Application of the slope (the b value) of the Gutenberg–Richter frequency–magnitude distribution to the spatiotemporal change in the seismicity revealed that the b value in the northern area increased significantly, the increase being $\Delta b = 0.3$–0.5. Significance was verified by a statistical test of Δb and a test using bootstrapping errors. Based on our findings, combined with the results obtained by a stress inversion analysis performed by the National Research Institute for Earth Science and Disaster Resilience, we suggested that stress near the Futagawa FZ had reduced just prior to the occurrence of the M7.3 quake. We proposed, with some other observations, that a reduction in stress might have been induced by growth of the slow slips on the Futagawa FZ.

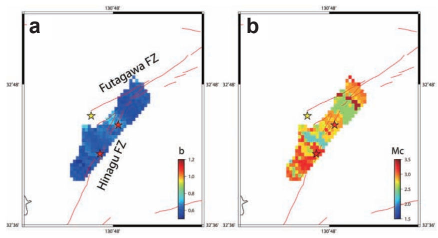

Figure 4

Keywords: The 2016 Kumamoto earthquakes, *p* value of the Omori–Utsu law, *b* value of the Gutenberg–Richter law, Hinagu fault zone, Futagawa fault zone, Slow slip

*Corresponding author: K. Z. Nanjo, nanjo@u-shizuoka-ken.ac.jp

FULL PAPER **Open Access**

Rupture process of the main shock of the 2016 Kumamoto earthquake with special reference to damaging ground motions: waveform inversion with empirical Green's functions

Atsushi Nozu* and Yosuke Nagasaka

Earth, Planets and Space 2017, **69**:22 doi:10.1186/s40623-017-0609-3
Received: 1 August 2016, Accepted: 24 January 2017, Published: 31 January 2017

Abstract

In this study, the rupture process of the main shock of the Kumamoto earthquake, particularly the generation of strong ground motions in the frequency range relevant to structural damage, was investigated based on the inversion of strong ground motions. Strong-motion records in the near-source region were mainly utilized because the authors were interested in the generation mechanism of damaging ground motions in the near-source region. Empirical Green's functions (EGFs) were applied to avoid uncertainty in the subsurface structure model. Four cases of inversions with different combinations of small events were used to investigate the dependence of the inversion results on the selection of the small events. It was found that the dependence of the final slip distribution and peak slip velocity distribution on the selection of the EGF events is small. The results clearly indicate that a region of significantly large slip and slip velocity existed approximately 15 km northeast of the hypocenter. However, no "asperity" was observed between the hypocenter and Mashiki. Thus, it is not appropriate to conclude that the large-amplitude pulse-like ground motion in Mashiki was generated by the forward-directivity effect associated with the rupture of an asperity. As far as the source effect is concerned, the ground motion in Mashiki cannot be interpreted as the worst case scenario. On the other hand, the rupture of the "asperity" 15 km northeast of the hypocenter should have caused significantly large ground motions in regions close to the asperity. The significant damage of highway bridges in the region can potentially be attributed to the rupture of the asperity. The result of this study was compared with an inversion result obtained from numerical Green's functions for a layered half-space. The two results share the main features in spite of the difference of the Green's functions and stations used. Therefore, it can be concluded that these two source models capture the main features of the rupture process of the earthquake.

Keywords: The 2016 Kumamoto earthquake, Rupture process, Strong ground motion, Waveform inversion, Empirical Green's function, Asperity, Forward directivity

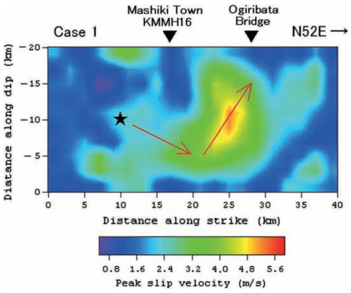

Figure 11

*Corresponding author: Atsushi Nozu, nozu@pari.go.jp

FULL PAPER **Open Access**

Strong ground motion simulation of the 2016 Kumamoto earthquake of April 16 using multiple point sources

Yosuke Nagasaka* and Atsushi Nozu

Earth, Planets and Space 2017, **69**:25 doi:10.1186/s40623-017-0612-8
Received: 1 August 2016, Accepted: 24 January 2017, Published: 2 February 2017

Abstract

The pseudo point-source model approximates the rupture process on faults with multiple point sources for simulating strong ground motions. A simulation with this point-source model is conducted by combining a simple source spectrum following the omega-square model with a path spectrum, an empirical site amplification factor, and phase characteristics. Realistic waveforms can be synthesized using the empirical site amplification factor and phase models even though the source model is simple. The Kumamoto earthquake occurred on April 16, 2016, with M_{JMA} 7.3. Many strong motions were recorded at stations around the source region. Some records were considered to be affected by the rupture directivity effect. This earthquake was suitable for investigating the applicability of the pseudo point-source model, the current version of which does not consider the rupture directivity effect. Three subevents (point sources) were located on the fault plane, and the parameters of the simulation were determined. The simulated results were compared with the observed records at K-NET and KiK-net stations. It was found that the synthetic Fourier spectra and velocity waveforms generally explained the characteristics of the observed records, except for underestimation in the low frequency range. Troughs in the observed Fourier spectra were also well reproduced by placing multiple subevents near the hypocenter. The underestimation is presumably due to the following two reasons. The first is that the pseudo point-source model targets subevents that generate strong ground motions and does not consider the shallow large slip. The second reason is that the current version of the pseudo point-source model does not consider the rupture directivity effect. Consequently, strong pulses were not reproduced enough at stations northeast of Subevent 3 such as KMM004, where the effect of rupture directivity was significant, while the amplitude was well reproduced at most of the other stations. This result indicates the necessity for improving the pseudo point-source model, by introducing azimuth-dependent corner frequency for example, so that it can incorporate the effect of rupture directivity.

Keywords: 2016 Kumamoto earthquake, Strong ground motion simulation, Pseudo point-source model, Rupture directivity

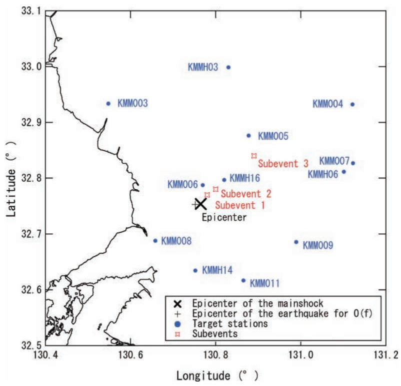

Figure 1

*Corresponding author: Yosuke Nagasaka, nagasaka-y@pari.go.jp

FULL PAPER Open Access

Data completeness of the Kumamoto earthquake sequence in the JMA catalog and its influence on the estimation of the ETAS parameters

Jiancang Zhuang*, Yosihiko Ogata and Ting Wang

Earth, Planets and Space 2017, **69**:36 doi:10.1186/s40623-017-0614-6
Received: 5 November 2016, Accepted: 31 January 2017, Published: 27 February 2017

Abstract

This study investigates the missing data problem in the Japan Meteorological Agency catalog of the Kumamoto aftershock sequence, which occurred since April 15, 2016, in Japan. Based on the assumption that earthquake magnitudes are independent of their occurrence times, we replenish the short-term missing data of small earthquakes by using a bi-scale transformation and study their influence on the maximum likelihood estimate (MLE) of the epidemic-type aftershock sequences (ETAS) parameters by comparing the analysis results from the original and the replenished datasets. The results show that the MLEs of the ETAS parameters vary when this model is fitted to the recorded catalog with different cutoff magnitudes, while those MLEs remain stable for the replenished dataset. Further analysis shows that the seismicity becomes quiescent after the occurrence of the second major shock, which can be regarded as a precursory phenomenon of the occurrence of the subsequent M_J7.3 mainshock. This relative quiescence is demonstrated more clearly by the analysis of the replenished dataset.

Keywords: Kumamoto earthquake, ETAS model, Missing data imputation, Relative quiescence, Short-term aftershock missing

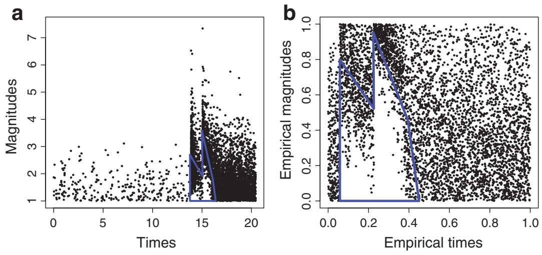

Figure 3

*Corresponding author: Jiancang Zhuang, zhuangjc@ism.ac.jp

FULL PAPER Open Access

Effects of the 2016 Kumamoto earthquakes on the Aso volcanic edifice

Yasuhisa Tajima*, Toshiaki Hasenaka and Masayuki Torii

Earth, Planets and Space 2017, **69**:63 doi:10.1186/s40623-017-0646-y
Received: 9 August 2016, Accepted: 14 April 2017, Published: 2 May 2017

Abstract

Large earthquakes occurred in the central part of Kumamoto Prefecture on April 14–16, 2016, causing severe damage to the northern segment of the Hinagu faults and the eastern segment of the Futagawa faults. Earthquake surface ruptures appeared along these faults and on the Aso volcanic edifice, which in turn generated landslides. We conducted landform change analysis of the central cones of Aso volcano by using satellite and aerial photographs. First, we categorized the topographical changes as surface scarps, arc-shaped cracks, and linear cracks. Field survey indicated that landslides caused the scarps and arc-shaped cracks, whereas faulting caused the linear cracks. We discovered a surface rupture concentration zone (RCZ) formed three ruptures bands with many surface ruptures and landslides extending from the west foot to the center of the Aso volcanic edifice. The magmatic volcanic vents that formed during the past 10,000 years are located along the north margin of the RCZ. Moreover, the distribution and dip of the core of rupture concentration zone correspond with the Nakadake craters. We conclude that a strong relationship exists between the volcanic vents and fault structures in the central cones of Aso volcano.

Keywords: Kumamoto earthquake, Surface rupture, Central cones of Aso volcano, Vent location, Magma plumbing system

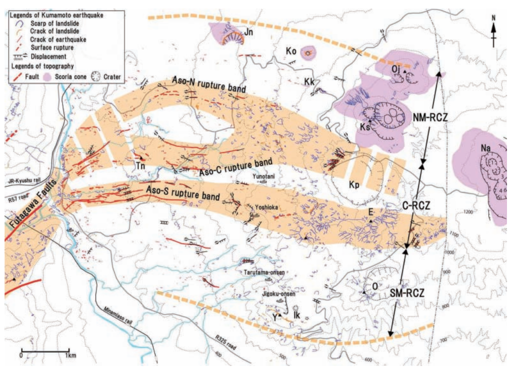

Figure 10

*Corresponding author: Yasuhisa Tajima, yasuhisa79@gmail.com

LETTER **Open Access**

Dip distribution of Oita–Kumamoto Tectonic Line located in central Kyushu, Japan, estimated by eigenvectors of gravity gradient tensor

Shigekazu Kusumoto

Earth, Planets and Space 2016, **68**:153 doi:10.1186/s40623-016-0529-7
Received: 17 June 2016, Accepted: 27 August 2016, Published: 6 September 2016

Abstract

We estimated the dip distribution of Oita–Kumamoto Tectonic Line located in central Kyushu, Japan, by using the dip of the maximum eigenvector of the gravity gradient tensor. A series of earthquakes in Kumamoto and Oita beginning on 14 April 2016 occurred along this tectonic line, the largest of which was $M = 7.3$. Because a gravity gradiometry survey has not been conducted in the study area, we calculated the gravity gradient tensor from the Bouguer gravity anomaly and employed it to the analysis. The general dip distribution of the Oita–Kumamoto Tectonic Line was found to be about 65° and tends to be higher towards its eastern end. In addition, we estimated the dip around the largest earthquake to be about 60° from the gravity gradient tensor. This result agrees with the dip of the earthquake source fault obtained by Global Navigation Satellite System data analysis.

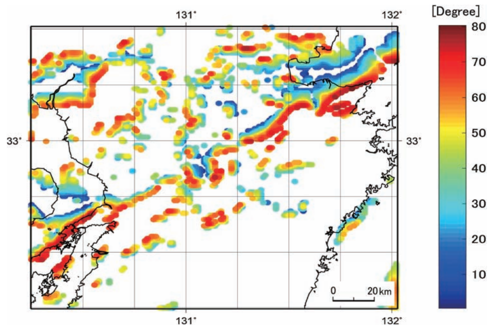

Figure 5

Keywords: Dip distribution, Oita–Kumamoto Tectonic Line, Kumamoto earthquake, Gravity gradient tensor, Eigenvector, Futagawa fault system, Aso caldera, Hohi volcanic zone

Corresponding author: Shigekazu Kusumoto, kusu@sci.u-toyama.ac.jp

LETTER **Open Access**

Source rupture processes of the 2016 Kumamoto, Japan, earthquakes estimated from strong-motion waveforms

Hisahiko Kubo*, Wataru Suzuki, Shin Aoi and Haruko Sekiguchi

Earth, Planets and Space 2016, **68**:161 doi:10.1186/s40623-016-0536-8
Received: 1 July 2016, Accepted: 19 September 2016, Published: 3 October 2016

Abstract

The detailed source rupture process of the *M* 7.3 event (April 16, 2016, 01:25, JST) of the 2016 Kumamoto, Japan, earthquakes was derived from strong-motion waveforms using multiple-time-window linear waveform inversion. Based on the observations of surface ruptures, the spatial distribution of aftershocks, and the geodetic data, a realistic curved fault model was developed for source-process analysis of this event. The seismic moment and maximum slip were estimated as 5.5×10^{19} Nm (M_w 7.1) and 3.8 m, respectively. The source model of the *M* 7.3 event had two significant ruptures. One rupture propagated toward the northeastern shallow region at 4 s after rupture initiation and continued with large slips to approximately 16 s. This rupture caused a large slip region 10–30 km northeast of the hypocenter that reached the caldera of Mt. Aso. Another rupture propagated toward the surface from the hypocenter at 2–6 s and then propagated toward the northeast along the near surface at 6–10 s. A comparison with the result of using a single fault plane model demonstrated that the use of the curved fault model led to improved waveform fit at the stations south of the fault. The source process of the *M* 6.5 event (April 14, 2016, 21:26, JST) was also estimated. In the source model obtained for the *M* 6.5 event, the seismic moment was 1.7×10^{18} Nm (M_w 6.1), and the rupture with large slips propagated from the hypocenter to the surface along the north-northeast direction at 1–6 s. The results in this study are consistent with observations of the surface ruptures.

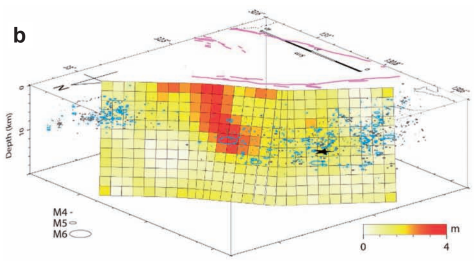

Figure 4

Keywords: The 2016 Kumamoto earthquakes, Source rupture process, Strong-motion waveforms

*Corresponding author: Hisahiko Kubo, hkubo@bosai.go.jp

LETTER Open Access

Continuity, segmentation and faulting type of active fault zones of the 2016 Kumamoto earthquake inferred from analyses of a gravity gradient tensor

Nayuta Matsumoto*, Yoshihiro Hiramatsu and Akihiro Sawada

Earth, Planets and Space 2016, **68**:167 doi:10.1186/s40623-016-0541-y
Received: 29 July 2016, Accepted: 6 October 2016, Published: 21 October 2016

Abstract

We analyze Bouguer anomalies in/around the focal region of the 2016 Kumamoto earthquake to examine features, such as continuity, segmentation and faulting type, of the active fault zones related to the earthquake. Several derivatives and structural parameters calculated from a gravity gradient tensor are applied to highlight the features. First horizontal and vertical derivatives, as well as a normalized total horizontal derivative, characterize well the continuous subsurface fault structure along the Futagawa fault zone. On the other hand, the Hinagu fault zone is not clearly detected by these derivatives, especially in the case of the Takano-Shirahata segment, suggesting a difference of cumulative vertical displacement between the two fault zones. The normalized total horizontal derivative and the dimensionality index indicate a discontinuity of the subsurface structure of the Hinagu fault zone, that is, a segment boundary between the Takano-Shirahata and the Hinagu segments. The aftershock distribution does not extend beyond this segment boundary. In other words, this segment boundary controls the southern end of the rupture area of the foreshock. We also recognize normal fault structures dipping to the northwest in some areas of the fault zones from estimations of dip angles.

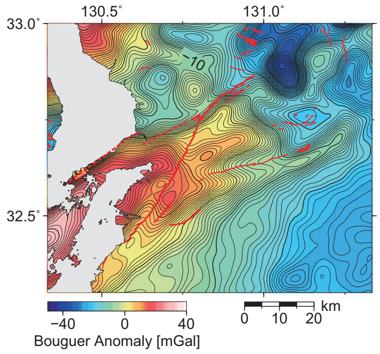

Figure 3

Keywords: First horizontal derivative, First vertical derivative, Normalized total horizontal derivative, Dip angle, Dimensionality index, Segment boundary, Aftershock distribution

*Corresponding author: Nayuta Matsumoto, n.matsumoto@stu.kanazawa-u.ac.jp

LETTER Open Access

Fault source model for the 2016 Kumamoto earthquake sequence based on ALOS-2/PALSAR-2 pixel-offset data: evidence for dynamic slip partitioning

Yuji Himematsu* and Masato Furuya

Earth, Planets and Space 2016, **68**:169 doi:10.1186/s40623-016-0545-7
Received: 21 July 2016, Accepted: 8 October 2016, Published: 22 October 2016

Abstract

Series of earthquakes including three $M_w > 6$ earthquakes occurred in Kumamoto prefecture in the middle of the Kyushu island, Japan. In order to reveal the associated crustal deformation signals, we applied offset tracking technique to ALOS-2/PALSAR-2 data covering three $M_w > 6$ earthquakes and derived the 3D displacements around the epicenters. We could identify three NE–SW trending displacement discontinuities in the 3D displacements that were consistent with the surface location of Futagawa and Hinagu fault system. We set three-segment fault model whose positions matched the displacement discontinuities, and estimated the slip distributions on each segment from the observed pixel-offset data. Whereas right-lateral slip was dominant in the shallower depth of the larger segments, normal fault slip was more significant at a greater depth of the other segment. The inferred configuration and slip distribution of each segment suggest that slip partitioning under oblique extension stress regime took place during the 2016 Kumamoto earthquake sequence. Moreover, given the consistent focal mechanisms derived from both the slip distribution model and seismology, the significant non-double couple components in the focal mechanism of the main shock are due to simultaneous ruptures of both strike-slip and normal faulting at the distinct segments.

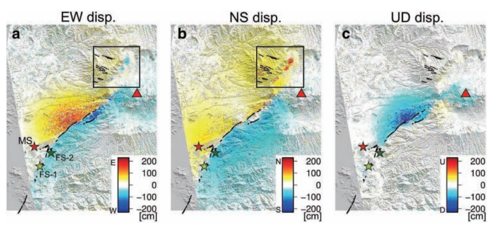

Figure 3

Keywords: ALOS-2/PALSAR-2, Offset tracking, Crustal deformation, Triangular dislocation element, Slip partitioning, Non-double couple component

*Corresponding author: Yuji Himematsu, hime.matsu@frontier.hokudai.ac.jp

LETTER **Open Access**

Surface fault ruptures associated with the 14 April foreshock (Mj 6.5) of the 2016 Kumamoto earthquake sequence, southwest Japan

Nobuhiko Sugito*, Hideaki Goto, Yasuhiro Kumahara, Hiroyuki Tsutsumi, Takashi Nakata, Kyoko Kagohara, Nobuhisa Matsuta and Haruka Yoshida

Earth, Planets and Space 2016, **68**:170 doi:10.1186/s40623-016-0547-5
Received: 30 July 2016, Accepted: 13 October 2016, Published: 3 November 2016

Abstract

The 2016 Kumamoto earthquake sequence was a rare event worldwide in that the surface ruptures associated with the largest foreshock (Mj 6.5) of 21:26 (JST), 14 April ruptured again during the mainshock (Mj 7.3) of 01:25 (JST), 16 April. The 14 April Mj 6.5 earthquake produced 6-km-long surface ruptures along the central portion of the Futagawa–Hinagu fault zone (FHFZ). The mainshock produced 31-km-long surface ruptures along the central to northeastern part of the FHFZ. Field observations and eyewitness accounts documented that the offsets of the ruptures associated with the 14 April foreshock became larger after the 16 April mainshock, suggesting that the same portion of the fault ruptured to the surface twice in the Kumamoto earthquake sequence. The 6-km-long surface ruptures associated with the largest foreshock are located near a geometric bend of the FHFZ characterized by ~50° change in strike. The epicenter of the mainshock is also located near the bend. These observations imply that the Kumamoto earthquake sequence was initiated due to a stress concentration on the bend of the FHFZ, and the mainshock was initiated approximately at the same place about 28 h after the largest foreshock. This foreshock/mainshock sequence of the Kumamoto earthquake is not successive events on the adjacent different fault zones, because the 6-km-long surface ruptures of the largest foreshock are part of the 31-km-long surface ruptures of the mainshock.

Keywords: 2016 Kumamoto earthquake sequence, Largest foreshock, Mainshock, Futagawa–Hinagu fault zone, Geometric bend, Surface ruptures

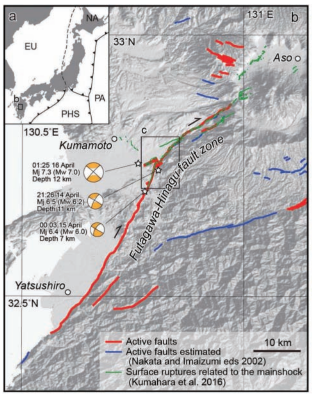

Figure 1

*Corresponding author: Nobuhiko Sugito, nsugito@hosei.ac.jp

LETTER **Open Access**

Earthquakes in Oita triggered by the 2016 *M*7.3 Kumamoto earthquake

Shingo Yoshida

Earth, Planets and Space 2016, **68**:176 doi:10.1186/s40623-016-0552-8
Received: 31 July 2016, Accepted: 26 October 2016, Published: 14 November 2016

Abstract

During the passage of the seismic waves from the *M*7.3 Kumamoto, Kyushu, earthquake on April 16, 2016, a *M*5.7 [semiofficial value estimated by the Japan Meteorological Agency (JMA)] event occurred in the central part of Oita prefecture, approximately 80 km far away from the mainshock. Although there have been a number of reports that $M < 5$ earthquakes were remotely triggered during the passage of seismic waves from mainshocks, there has been no evidence for $M > 5$ triggered events. In this paper, we firstly confirm that this event is a *M*6-class event by re-estimating the magnitude using the strong-motion records of K-NET and KiK-net, and crustal deformation data at the Yufuin station observed by the Geospatial Information Authority of Japan. Next, by investigating the aftershocks of 45 mainshocks which occurred over the past 20 years based on the JMA earthquake catalog (JMAEC), we found that the delay time of the 2016 *M*5.7 event in Oita was the shortest. Therefore, the *M*5.7 event could be regarded as an exceptional $M > 5$ event that was triggered by passing seismic waves, unlike the usual triggered events and aftershocks. Moreover, a search of the JMAEC shows that in the 2016 Oita aftershock area, swarm earthquake activity was low over the past 30 years compared with neighboring areas. We also found that in the past, probably or possibly triggered events frequently occurred in the 2016 Oita aftershock area. The Oita area readily responds to remote triggering because of high geothermal activity and young volcanism in the area. The *M*5.7 Oita event was triggered by passing seismic waves, probably because large dynamic stress change was generated by the mainshock at a short distance and because the Oita area was already loaded to a critical stress state without a recent energy release as suggested by the past low swarm activity.

Keywords: Dynamic earthquake triggering, Aftershocks in Oita, The 2016 Kumamoto earthquake

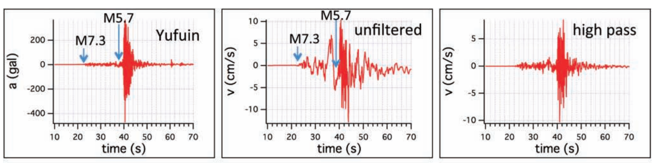

Figure 2

Corresponding author: Shingo Yoshida, shingo@eri.u-tokyo.ac.jp

LETTER Open Access

Crustal deformation model of the Beppu–Shimabara graben area, central Kyushu, Japan, based on inversion of three-component GNSS data in 2000–2010

Kazuma Mochizuki and Yuta Mitsui*

Earth, Planets and Space 2016, **68**:177 doi:10.1186/s40623-016-0550-x
Received: 26 July 2016, Accepted: 18 October 2016, Published: 11 November 2016

Abstract

The 2016 Kumamoto earthquakes, including an Mw-7 right-lateral earthquake on April 15 (UTC), occurred along faults within the Beppu–Shimabara graben in central Kyushu, Japan. Previous studies showed that the graben area was under heterogeneous stress conditions with north–south *T*-axes and spreading in a north–south direction. Here, we construct a detailed crustal deformation model using three-component Global Navigation Satellite System data in 2000–2010 and considering the distribution of geological fault traces in this area. Our inversion analysis suggests that the strain accumulation rate for the right-lateral seismic slip segment (corresponding to the Futagawa fault), where the largest of the 2016 Kumamoto earthquakes ruptured, was several times smaller than the other segments in the Beppu–Shimabara graben. Furthermore, we observe distinct subsidence along the Beppu–Shimabara graben. Our base model attributes the subsidence to deflation of magma reservoirs beneath volcanoes, but the observed vertical velocities are poorly fit. In order to improve the fitting results for the vertical deformation, we need more sophisticated volcano-deformation model (such as a sill-like deformation source for Mt. Aso) or graben model.

Keywords: The 2016 Kumamoto earthquakes, Kyushu, GNSS, Crustal deformation, Beppu–Shimabara graben, Volcano, Block-fault model, Nucleation

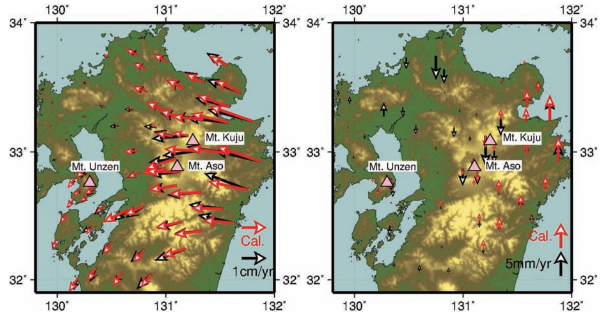

Figure 6

*Corresponding author: Yuta Mitsui, mit@shizuoka.ac.jp

LETTER Open Access

The 2016 Kumamoto–Oita earthquake sequence: aftershock seismicity gap and dynamic triggering in volcanic areas

Takahiko Uchide*, Haruo Horikawa, Misato Nakai, Reiken Matsushita, Norio Shigematsu, Ryosuke Ando and Kazutoshi Imanishi

Earth, Planets and Space 2016, **68**:180 doi:10.1186/s40623-016-0556-4
Received: 22 July 2016, Accepted: 29 October 2016, Published: 15 November 2016

Abstract

The 2016 Kumamoto–Oita earthquake sequence involving three large events ($M_w \geq 6$) in the central Kyushu Island, southwest Japan, activated seismicities in two volcanic areas with unusual and puzzling spatial gaps after the largest earthquake (M_w 7.0) of April 16, 2016. We attempt to reveal the seismic process during the sequence by following seismological data analyses. Our hypocenter relocation result implies that the large events ruptured different faults of a complex fault system. A slip inversion analysis of the largest event indicates a large slip in the seismicity gap (Aso gap) in the caldera of Mt. Aso, which probably released accumulated stress and resulted in little aftershock production. We identified that the largest event dynamically triggered a mid-M6 event at Yufuin (80 km northeast of the epicenter), which is consistent with existence of the 20-km long zone where seismicity was activated and surface offset was observed. These findings will help us study the contribution of the identified complexity in fault geometries and the geotherm in the volcanic areas to the revealed seismic process and consequently improve our understanding of the seismo-volcano tectonics.

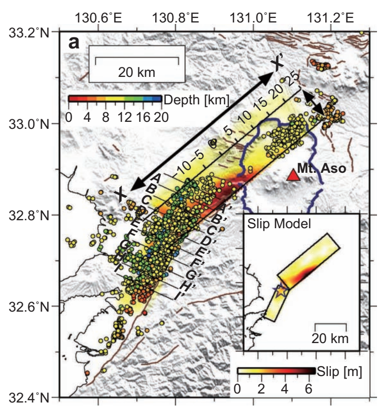

Figure 3

*Corresponding author: Takahiko Uchide, t.uchide@aist.go.jp

LETTER **Open Access**

Characteristics of the surface ruptures associated with the 2016 Kumamoto earthquake sequence, central Kyushu, Japan

Yoshiki Shirahama*, Masayuki Yoshimi, Yasuo Awata, Tadashi Maruyama, Takashi Azuma, Yukari Miyashita, Hiroshi Mori, Kazutoshi Imanishi, Naoto Takeda, Tadafumi Ochi, Makoto Otsubo, Daisuke Asahina and Ayumu Miyakawa

Earth, Planets and Space 2016, **68**:191 doi:10.1186/s40623-016-0559-1
Received: 31 July 2016, Accepted: 29 October 2016, Published: 24 November 2016

Abstract

The 2016 Kumamoto earthquake sequence started with a M_J (Japan Meteorological Agency magnitude) 6.5 event on April 14, and culminated in a M_J 7.3 event on April 16. Associated with the sequence, approximately 34-km-long surface ruptures appeared along the eastern part of the Futagawa fault zone and the northernmost part of the Hinagu fault zone. We carried out an urgent field investigation soon after the earthquake to map the extent and displacement of surface ruptures with the following results. (1) The rupture zone generally consisted of a series of left-stepping en echelon arrays of discontinuous fault traces of various lengths. (2) Slip exceeding 100 cm occurred on previously unrecognized fault traces in the alluvial lowland of the Kiyama plain and on the western rim of the Aso volcano caldera. (3) Large slip with maximum dextral slip of 220 cm was measured throughout the central section of the rupture zone along the Futagawa segment, and the slip gradually decreased bilaterally on the adjoining northeastern and southwestern sections. (4) The surface rupture mostly occurred along fault traces mapped in previous active fault investigations. (5) Most of the surface ruptures were produced by the mainshock, and significant postseismic slip occurred after the mainshock.

Keywords: 2016 Kumamoto earthquake surface rupture, Futagawa fault zone, Hinagu fault zone, Slip distribution, Urgent field investigation

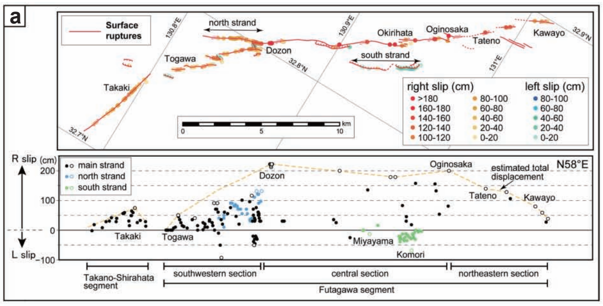

Figure 6

*Corresponding author: Yoshiki Shirahama, y.shirahama@aist.go.jp

LETTER **Open Access**

Near-fault deformation and Dc" during the 2016 Mw7.1 Kumamoto earthquake

Eiichi Fukuyama* and Wataru Suzuki

Earth, Planets and Space 2016, **68**:194 doi:10.1186/s40623-016-0570-6
Received: 29 June 2016, Accepted: 17 November 2016, Published: 29 November 2016

Abstract

An Mw7.1 Kumamoto earthquake occurred at 01:25:05 on April 16, 2016 (JST). The earthquake involved a rupture at a shallow depth along a strike-slip fault with surface breaks. Near-fault ground motion records, especially those of a strike-slip earthquake, can provide us with direct information on the earthquake source process. During the earthquake, near-fault seismograms were obtained at KMMH16 station located about 500 m off the fault. The ground displacements were well recovered from the double numerical integration of accelerograms at KMMH16 both on the surface and at the bottom of the 252-m-deep borehole. Fault-parallel static displacement was estimated to be about 1.1 m from the acceleration waveforms. The Dc" value, which is defined as double the fault-parallel displacement at peak velocity time, was proposed as a proxy of the slip-weakening distance. Using both the velocity and displacement fault-parallel waveforms, the Dc" value was estimated at about 1 m. This value was between 30 and 50% of the total slip on the fault, which is consistent with previous observations.

Keywords: Near-fault displacement, Slip-weakening distance, Strike-slip fault

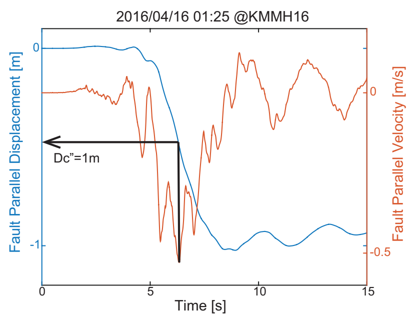

Figure 4

*Corresponding author: Eiichi Fukuyama, fuku@bosai.go.jp

LETTER Open Access

Observation of earthquake ground motion due to aftershocks of the 2016 Kumamoto earthquake in damaged areas

Hiroaki Yamanaka*, Kosuke Chimoto, Hiroe Miyake, Seiji Tsuno and Nobuyuki Yamada

Earth, Planets and Space 2016, **68**:197 doi:10.1186/s40623-016-0574-2
Received: 3 July 2016, Accepted: 22 November 2016, Published: 1 December 2016

Abstract

We have conducted observation of earthquake ground motion due to aftershocks of the 2016 Kumamoto earthquake at 26 temporary stations in damaged areas of Kumamoto city, Mashiki town, Nishihara village and Minami-Aso village (partly in Aso city) in Kumamoto prefecture, Japan. Continuous recordings of ground acceleration were acquired in a period of about 1 month after the occurrence of the main shock on April 16, 2016. This preliminary analysis of the observed records clearly indicates strong effects of local geological condition in the heavily damaged districts in Mashiki town and Nishihara village. Spectral ratios of the ground motions at the stations in the severely damaged districts to those at the reference sites are characterized by large amplitudes at periods of 0.5–1 s. Peak ground velocities and seismic intensities are also large at the sites. Seismic intensities at the stations in the damaged districts are larger by an intensity of one at the maximum than those at the stations with the minor damage. The ground motions at the stations in Kumamoto city are rich in later phases with long duration suggesting basin effects. However, site amplification effects could not clearly be identified at the stations in the Minami-Aso area from the results in the conventional spectral ratio approach.

Keywords: The 2016 Kumamoto earthquake, Aftershock, Earthquake ground motion, Strong motion observation, Site amplification

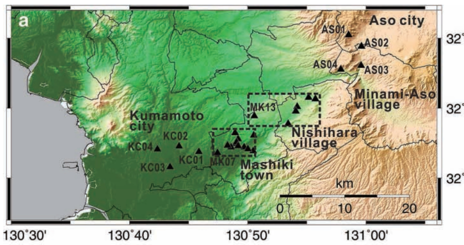

Figure 1

*Corresponding author: Hiroaki Yamanaka, yamanaka.h.aa@m.titech.ac.jp

LETTER Open Access

Ground motion estimation for the elevated bridges of the Kyushu Shinkansen derailment caused by the foreshock of the 2016 Kumamoto earthquake based on the site-effect substitution method

Yoshiya Hata*, Masaaki Yabe, Akira Kasai, Hiroshi Matsuzaki, Yoshikazu Takahashi and Mitsuyoshi Akiyama

Earth, Planets and Space 2016, **68**:199 doi:10.1186/s40623-016-0573-3
Received: 11 July 2016, Accepted: 19 November 2016, Published: 1 December 2016

Abstract

An earthquake of JMA magnitude 6.5 (first event) hit Kumamoto Prefecture, Japan, at 21:26 JST, April 14, 2016. Subsequently, an earthquake of JMA magnitude 7.3 (second event) hit Kumamoto and Oita Prefectures at 01:46 JST, April 16, 2016. An out-of-service Kyushu Shinkansen train carrying no passengers traveling on elevated bridges was derailed by the first event. This was the third derailment caused by an earthquake in the history of the Japanese Shinkansen, after one caused by the 2004 Mid-Niigata Prefecture Earthquake and another triggered by the 2011 Tohoku Earthquake. To analyze the mechanism of this third derailment, it is crucial to evaluate the strong ground motion at the derailment site with high accuracy. For this study, temporary earthquake observations were first carried out at a location near the bridge site; these observations were conducted because although the JMA Kumamoto Station site and the derailment site are closely located, the ground response characteristics at these sites differ. Next, empirical site amplification and phase effects were evaluated based on the obtained observation records. Finally, seismic waveforms during the first event at the bridge site of interest were estimated based on the site-effect substitution method. The resulting estimated acceleration and velocity waveforms for the derailment site include much larger amplitudes than the waveforms recorded at the JMA Kumamoto and MLIT Kumamoto station sites. The reliability of these estimates is confirmed by the finding that the same methods reproduce strong ground motions at the MLIT Kumamoto Station site accurately. These estimated ground motions will be useful for reasonable safety assessment of anti-derailment devices on elevated railway bridges.

Keywords: Seismic observation, Site-effect, Response spectrum

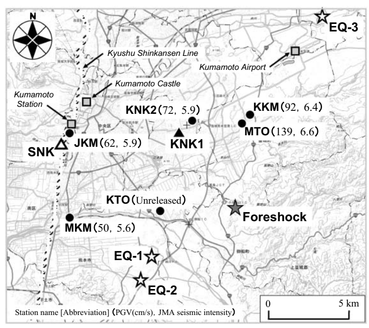

Figure 1

*Corresponding author: Yoshiya Hata, hata@civil.eng.osaka-u.ac.jp

LETTER **Open Access**

An investigation into the remote triggering of the Oita earthquake by the 2016 Mw 7.0 Kumamoto earthquake using full wavefield simulation

Masatoshi Miyazawa

Earth, Planets and Space 2016, **68**:205 doi:10.1186/s40623-016-0585-z
Received: 21 July 2016, Accepted: 6 December 2016, Published: 19 December 2016

Abstract

High-amplitude seismic waves from the Mw 7.0 Kumamoto earthquake of April 16, 2016, triggered another large earthquake 80 km to the NE roughly 30 s later. The source was located at shallow depths beneath the Yufuin geothermal field, Oita Prefecture, Japan, and the event magnitude was approximately 5.9. To date, this is one of the clearest known examples of a remotely triggered large earthquake. The triggered Oita event was followed by significant seismicity, which was distinct from the aftershocks of the Kumamoto earthquake. The Coulomb failure stress change around the hypocenter, calculated for the passing waves of the Kumamoto earthquake by full wavefield simulation, was about 0.7 MPa when the Oita earthquake was triggered, with the static stress change being an order of magnitude smaller. The dynamic stress changes likely played an important role in triggering. A return to low seismicity levels 1 month after the triggered earthquake may have important implications for seismic hazard due to dynamic triggering.

Keywords: 2016 Kumamoto earthquake, Remote triggering, Coulomb failure stress change, Wavefield simulation

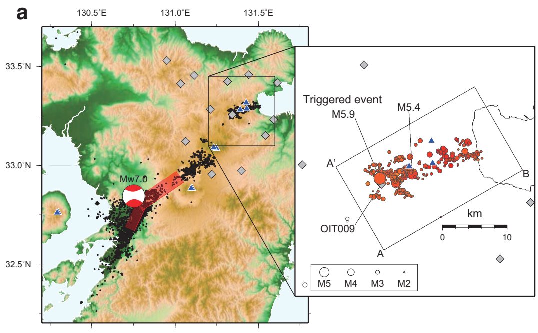

Figure 3

Corresponding author: Masatoshi Miyazawa, miyazawa@rcep.dpri.kyoto-u.ac.jp

LETTER **Open Access**

Estimation of shallow S-wave velocity structure using microtremor array exploration at temporary strong motion observation stations for aftershocks of the 2016 Kumamoto earthquake

Kosuke Chimoto*, Hiroaki Yamanaka, Seiji Tsuno, Hiroe Miyake and Nobuyuki Yamada

Earth, Planets and Space 2016, **68**:206 doi:10.1186/s40623-016-0581-3
Received: 29 July 2016, Accepted: 3 December 2016, Published: 19 December 2016

Abstract

Shallow S-wave velocity V_S profiles were estimated for 26 temporary strong motion observation sites surrounding the epicenters of a sequence of the 2016 Kumamoto earthquake. The microtremor array method was used to gather the dispersion characteristics of Rayleigh waves. V_S profiles were obtained by inverting the dispersion curves for each site and those of three permanent strong motion stations that recorded the sequence of seismic events. The shallow V_S profiles near two of the permanent strong motion stations in the town of Mashiki were almost identical. However, the V_S profiles at other stations varied. The V_S profiles were found to have the common feature of the uppermost low-velocity layer being widely distributed from Mashiki to the village of Minami-Aso, and it was especially thick in the areas that suffered heavy damage. This low-velocity layer was a major contributor to the site amplification. The horizontal-to-vertical spectral ratios of the microtremors indicate that both the shallow soil and deep sedimentary layers may control the site response characteristics over a broad frequency range.

Keywords: Shallow S-wave velocity structure, Microtremor array exploration, 2016 Kumamoto earthquake, Site amplification

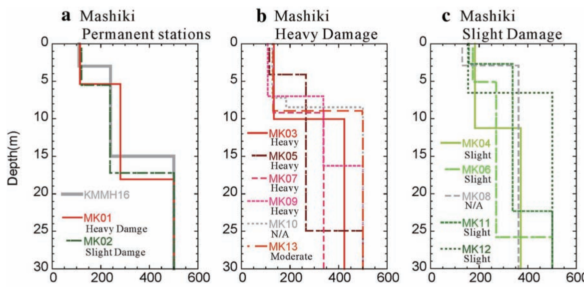

Figure 4

*Corresponding author: Kosuke Chimoto, chimoto.k.aa@m.titech.ac.jp

LETTER **Open Access**

Inelastic strain rate in the seismogenic layer of Kyushu Island, Japan

Satoshi Matsumoto*, Takuya Nishimura and Takahiro Ohkura

Earth, Planets and Space 2016, **68**:207 doi:10.1186/s40623-016-0584-0
Received: 7 July 2016, Accepted: 3 December 2016, Published: 28 December 2016

Abstract

Seismic activity is associated with crustal stress relaxation, creating inelastic strain in a medium due to faulting. Inelastic strain affects the stress field around a weak body and causes stress concentration around the body, because the body itself has already released stress. Therefore, the understanding of inelastic deformation is important as it generates earthquakes. We investigated average inelastic strain in a spatial bin of Kyushu Island, Japan, and obtained the inelastic strain rate distribution associated with crustal earthquakes, based on the analysis of fault plane solutions and seismic moments. Large inelastic strains (>10^{-7} year^{-1}) were found in the Beppu–Shimabara area, located in the center of Kyushu Island. The strain rate tensor was similar to that of the stress tensor except the absolute value in the area, implying that the inelastic strain was controlled by the stress field. The 2016 Kumamoto earthquake sequence (maximum magnitude 7.3) occurred in the Beppu–Shimabara area, with the major earthquakes located around the high inelastic strain rate area. Inelastic strain in the volume released the stress. In addition, the inelastic strain created an increment of stress around the volume. This indicates that the spatial heterogeneity of inelastic strain might concentrate stress.

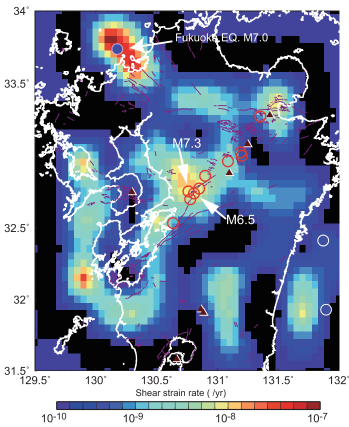

Figure 5

Keywords: Inelastic strain field, Kyushu, Moment tensor, Seismogenic zone

*Corresponding author: Satoshi Matsumoto, matumoto@sevo.kyushu-u.ac.jp

LETTER **Open Access**

Volcanic magma reservoir imaged as a low-density body beneath Aso volcano that terminated the 2016 Kumamoto earthquake rupture

Ayumu Miyakawa*, Tatsuya Sumita, Yasukuni Okubo, Ryo Okuwaki, Makoto Otsubo, Shimpei Uesawa and Yuji Yagi

Earth, Planets and Space 2016, **68**:208 doi:10.1186/s40623-016-0582-2
Received: 9 July 2016, Accepted: 3 December 2016, Published: 30 December 2016

Abstract

We resolve the density structure of a possible magma reservoir beneath Aso, an active volcano on Kyushu Island, Japan, by inverting gravity data. In the context of the resolved structure, we discuss the relationship between the fault rupture of the 2016 Kumamoto earthquake and Aso volcano. Low-density bodies were resolved beneath central Aso volcano using a three-dimensional inversion with an assumed density contrast of ±0.3 g/cm^3. The resultant location of the southern low-density body is consistent with a magma reservoir reported in previous studies. No Kumamoto aftershocks occur in the southern low-density body; this aseismic anomaly may indicate a ductile feature due to high temperatures and/or the presence of partial melt. Comparisons of the location of the southern low-density body with rupture models of the mainshock, obtained from teleseismic waveform and InSAR data, suggest that the rupture terminus overlaps the southern low-density body. The ductile features of a magma reservoir could have terminated rupture propagation. On the other hand, a northern low-density body is resolved in the Asodani area, where evidence of current volcanic activity is scarce and aftershock activity is high. The northern low-density body might, therefore, be derived from a thick caldera fill in the Asodani area, or correspond to mush magma or a high-crystallinity magma reservoir that could be the remnant of an ancient intrusion.

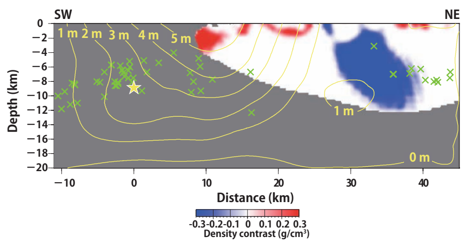

Figure 4

Keywords: 2016 Kumamoto earthquake, Density structure, Gravity inversion, Volcano-tectonic interactions

*Corresponding author: Ayumu Miyakawa, miyakawa-a@aist.go.jp

LETTER **Open Access**

The cause of heavy damage concentration in downtown Mashiki inferred from observed data and field survey of the 2016 Kumamoto earthquake

Hiroshi Kawase*, Shinichi Matsushima, Fumiaki Nagashima, Baoyintu and Kenichi Nakano

Earth, Planets and Space 2017, **69**:3 doi:10.1186/s40623-016-0591-1
Received: 31 July 2016, Accepted: 17 December 2016, Published: 3 January 2017

Abstract

To understand the cause of heavy structural damage during the mainshock (on April 16, 2016) of the 2016 Kumamoto earthquake sequence, we carried out a field survey from April 29 through May 1, 2016, in Mashiki where heavy damage concentration was observed. The heavy damage concentration in downtown Mashiki could be understood based on the observed strong motions with the Japan Meteorological Agency instrumental seismic intensity of VII and information collected by the field investigation. First, the fundamental features of the structural damage in downtown Mashiki were summarized. Then, a distribution map of peak frequencies was derived from horizontal-to-vertical spectral ratios of microtremors. We could not see any systematic correlation between the peak frequencies and spatial distribution of damage ratios. We also analyzed observed strong motion data at two sites to obtain fling-step-like motions in the displacement time histories through the double integration of unfiltered accelerograms. It turned out that at both strong motion observation sites in Mashiki, only the east–west (EW) components had very strong velocity pulses westward before the emergence of the fling-step-like motion eastward, which would be the primary cause of heavy structural damage in downtown Mashiki, not site effects nor the fling-step-like motion itself.

Keywords: Structural damage, HVR, Site effects, Fling-step, Directivity

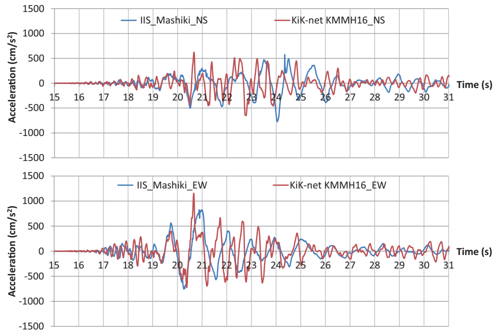

Figure 9

*Corresponding author: Hiroshi Kawase, kawase@zeisei.dpri.kyoto-u.ac.jp

LETTER **Open Access**

Seismicity controlled by resistivity structure: the 2016 Kumamoto earthquakes, Kyushu Island, Japan

Koki Aizawa*, Hisafumi Asaue, Katsuaki Koike, Shinichi Takakura, Mitsuru Utsugi, Hiroyuki Inoue, Ryokei Yoshimura, Ken'ichi Yamazaki, Shintaro Komatsu, Makoto Uyeshima, Takao Koyama, Wataru Kanda, Taro Shiotani, Nobuo Matsushima, Maki Hata, Tohru Yoshinaga, Kazunari Uchida, Yuko Tsukashima, Azusa Shito, Shiori Fujita, Asuma Wakabayashi, Kaori Tsukamoto, Takeshi Matsushima, Masahiro Miyazaki, Kentaro Kondo, Kanade Takashima, Takeshi Hashimoto, Makoto Tamura, Satoshi Matsumoto, Yusuke Yamashita, Manami Nakamoto and Hiroshi Shimizu

Earth, Planets and Space 2017, **69**:4 doi:10.1186/s40623-016-0590-2
Received: 29 July 2016, Accepted: 17 December 2016, Published: 3 January 2017

Abstract

The M_{JMA} 7.3 Kumamoto earthquake that occurred at 1:25 JST on April 16, 2016, not only triggered aftershocks in the vicinity of the epicenter, but also triggered earthquakes that were 50–100 km away from the epicenter of the main shock. The active seismicity can be divided into three regions: (1) the vicinity of the main faults, (2) the northern region of Aso volcano (50 km northeast of the mainshock epicenter), and (3) the regions around three volcanoes, Yufu, Tsurumi, and Garan (100 km northeast of the mainshock epicenter). Notably, the zones between these regions are distinctively seismically inactive. The electric resistivity structure estimated from one-dimensional analysis of the 247 broadband (0.005–3000 s) magnetotelluric and telluric observation sites clearly shows that the earthquakes occurred in resistive regions adjacent to conductive zones or resistive-conductive transition zones. In contrast, seismicity is quite low in electrically conductive zones, which are interpreted as regions of connected fluids. We suggest that the series of the earthquakes was induced by a local accumulated stress and/or fluid supply from conductive zones. Because the relationship between the earthquakes and the resistivity structure is consistent with previous studies, seismic hazard assessment generally can be improved by taking into account the resistivity structure. Following on from the 2016 Kumamoto earthquake series, we suggest that there are two zones that have a relatively high potential of earthquake generation along the western extension of the MTL.

Keywords: Magnetotellurics, Resistivity structure, 2016 Kumamoto earthquake, Futagawa fault, Hinagu fault, Structural control, Aso volcano, Kuju volcano, Tsurumi volcano, Median Tectonic Line

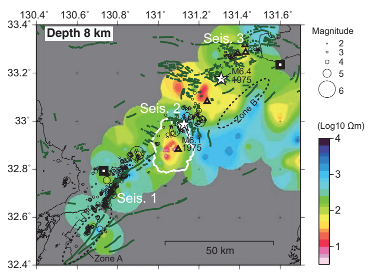

Figure 6

*Corresponding author: Koki Aizawa, aizawa@sevo.kyushu-u.ac.jp

LETTER Open Access

Source location and mechanism analysis of an earthquake triggered by the 2016 Kumamoto, southwestern Japan, earthquake

Takeshi Nakamura* and Shin Aoi

Earth, Planets and Space 2017, **69**:6 doi:10.1186/s40623-016-0588-9
Received: 1 August 2016, Accepted: 9 December 2016, Published: 3 January 2017

Abstract

The 2016 Kumamoto earthquake (*M*w 7.0) occurred in the central part of Kyushu Island, southwestern Japan, on April 16, 2016. The mainshock triggered an event of maximum acceleration 700 gal that caused severe damage to infrastructure and thousands of homes. We investigate the source location of the triggered event, and the timing of large energy release, by employing the back-projection method for strong-motion network data. The optimal location is estimated to be [33.2750°, 131.3575°] (latitude, longitude) at a depth of 5 km, which is 80 km northeast of the epicenter of the mainshock. The timing is 33.5 s after the origin time of the mainshock. We also investigate the source mechanism by reproducing observed displacement waveforms at a near-source station. The waveforms at smaller-sized events, convolved with the source time function of a pulse width 1 s, are similar to the signature of the observed waveforms of the triggered event. The observations are also reproduced by synthetic waveforms for a normal-fault mechanism and a normal-fault with strike-slip components at the estimated locations. Although our approach does not constrain the strike direction well, our waveform analysis indicates that the triggered earthquake occurred near the station that observed the strong motions, primarily via a normal-fault mechanism or a normal-fault with strike-slip components.

Keywords: 2016 Kumamoto earthquake, Triggered earthquake, Strong motion, Back-projection method, Green's function, Hypocenter determination, Source mechanism

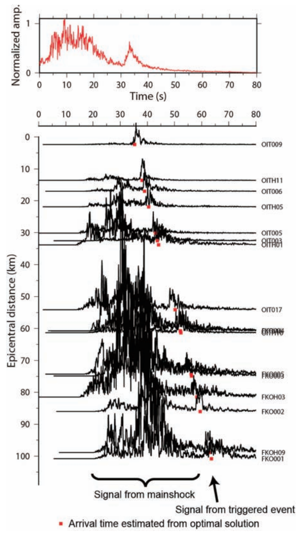

Figure 4

*Corresponding author: Takeshi Nakamura, t_nakamura@bosai.go.jp

LETTER Open Access

Earthquake rupture properties of the 2016 Kumamoto earthquake foreshocks (M_j 6.5 and M_j 6.4) revealed by conventional and multiple-aperture InSAR

Tomokazu Kobayashi

Earth, Planets and Space 2017, **69**:7 doi:10.1186/s40623-016-0594-y
Received: 5 July 2016, Accepted: 20 December 2016, Published: 3 January 2017

Abstract

By applying conventional cross-track InSAR and multiple-aperture InSAR (MAI) techniques with ALOS-2 SAR data to foreshocks of the 2016 Kumamoto earthquake, ground displacement fields in range (line-of-sight) and azimuth components have been successfully mapped. The most concentrated crustal deformation with ground displacement exceeding 15 cm is located on the western side of the Hinagu fault zone. A locally distributed displacement which appears along the strike of the Futagawa fault can be identified in and around Mashiki town, suggesting that a different local fault slip also contributed toward foreshocks. Inverting InSAR, MAI, and GNSS data, distributed slip models are obtained that show almost pure right-lateral fault motion on a plane dipping west by 80° for the Hinagu fault and almost pure normal fault motion on a plane dipping south by 70° for the local fault beneath Mashiki town. The slip on the Hinagu fault reaches around the junction of the Hinagu and Futagawa faults. The slip in the north significantly extends down to around 10 km depth, while in the south the slip is concentrated near the ground surface, perhaps corresponding to the M_j 6.5 and the M_j 6.4 events, respectively. The focal mechanism of the distributed slip model for the Hinagu fault alone shows pure right-lateral motion, which is inconsistent with the seismically estimated mechanism that includes a significant non-double couple component. On the other hand, when taking the contribution of normal fault motion into account, the focal mechanism appears similar to that of the seismic analysis. This result may suggest that local fault motion occurred just beneath Mashiki town, simultaneously with the M_j 6.5 event, thereby increasing the degree of damage to the town.

Keywords: Foreshocks, Kumamoto earthquake, InSAR, MAI, Crustal deformation, Fault model

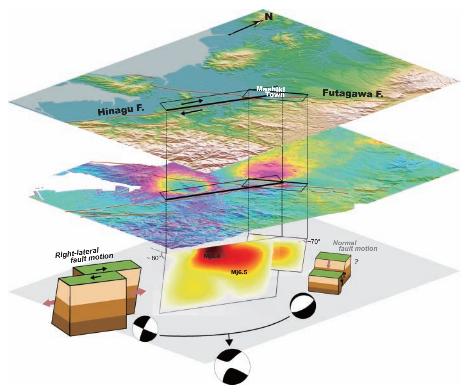

Figure 5

Corresponding author: Tomokazu Kobayashi, kobayashi-t96dv@mlit.go.jp

LETTER **Open Access**

Strong motions observed by K-NET and KiK-net during the 2016 Kumamoto earthquake sequence

Wataru Suzuki*, Shin Aoi, Takashi Kunugi, Hisahiko Kubo, Nobuyuki Morikawa, Hiromitsu Nakamura, Takeshi Kimura and Hiroyuki Fujiwara

Earth, Planets and Space 2017, **69**:19 doi:10.1186/s40623-017-0604-8
Received: 1 August 2016, Accepted: 14 January 2017, Published: 30 January 2017

Abstract

The nationwide strong-motion seismograph network of K-NET and KiK-net in Japan successfully recorded the strong ground motions of the 2016 Kumamoto earthquake sequence, which show the several notable characteristics. For the first large earthquake with a JMA magnitude of 6.5 (21:26, April 14, 2016, JST), the large strong motions are concentrated near the epicenter and the strong-motion attenuations are well predicted by the empirical relation for crustal earthquakes with a moment magnitude of 6.1. For the largest earthquake of the sequence with a JMA magnitude of 7.3 (01:25, April 16, 2016, JST), the large peak ground accelerations and velocities extend from the epicentral area to the northeast direction. The attenuation feature of peak ground accelerations generally follows the empirical relation, whereas that for velocities deviates from the empirical relation for stations with the epicentral distance of greater than 200 km, which can be attributed to the large Love wave having a dominant period around 10 s. The large accelerations were observed at stations even in Oita region, more than 70 km northeast from the epicenter. They are attributed to the local induced earthquake in Oita region, whose moment magnitude is estimated to be 5.5 by matching the amplitudes of the corresponding phases with the empirical attenuation relation. The real-time strong-motion observation has a potential for contributing to the mitigation of the ongoing earthquake disasters. We test a methodology to forecast the regions to be exposed to the large shaking in real time, which has been developed based on the fact that the neighboring stations are already shaken, for the largest event of the Kumamoto earthquakes, and demonstrate that it is simple but effective to quickly make warning. We also shows that the interpolation of the strong motions in real time is feasible, which will be utilized for the real-time forecast of ground motions based on the observed shakings.

Keywords: 2016 Kumamoto earthquake, Strong motion, PGA, PGV, Attenuation relation, Record section, Induced earthquake, Earthquake early warning, Real-time interpolation

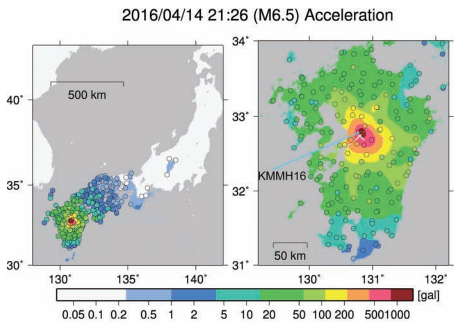

Figure 1

*Corresponding author: Wataru Suzuki, wsuzuki@bosai.go.jp

LETTER **Open Access**

Geomorphic features of surface ruptures associated with the 2016 Kumamoto earthquake in and around the downtown of Kumamoto City, and implications on triggered slip along active faults

Hideaki Goto*, Hiroyuki Tsutsumi, Shinji Toda and Yasuhiro Kumahara

Earth, Planets and Space 2017, **69**:26 doi:10.1186/s40623-017-0603-9
Received: 31 July 2016, Accepted: 14 January 2017, Published: 2 February 2017

Abstract

The ~30-km-long surface ruptures associated with the M_w 7.0 (M_j 7.3) earthquake at 01:25 JST on April 16 in Kumamoto Prefecture appeared along the previously mapped ~100-km-long active fault called the Futagawa-Hinagu fault zone (FHFZ). The surface ruptures appeared to have extended further west out of the main FHFZ into the Kumamoto Plain. Although InSAR analysis by Geospatial Information Authority of Japan (GSI) indicated coseismic surface deformation in and around the downtown of Kumamoto City, the surface ruptures have not been clearly mapped in the central part of the Kumamoto Plain, and whether there are other active faults other than the Futagawa fault in the Kumamoto Plain remained unclear. We produced topographical stereo images (anaglyph) from 5-m-mesh digital elevation model of GSI, which was generated from light detection and ranging data. We interpreted them and identified that several SW-sloping river terraces formed after the deposition of the pyroclastic flow deposits related to the latest large eruption of the Aso caldera (86.8–87.3 ka) are cut and deformed by several NW-trending flexure scarps down to the southwest. These 5.4-km-long scarps that cut across downtown Kumamoto were identified for the first time, and we name them as the Suizenji fault zone. Surface deformation such as continuous cracks, tilts, and monoclinal folding associated with the main shock of the 2016 Kumamoto earthquake was observed in the field along the fault zone. The amount of vertical deformation (~0.1 m) along this fault associated with the 2016 Kumamoto earthquake was quite small compared to the empirically calculated coseismic slip (0.5 m) based on the fault length. We thus suggest that the slip on this fault zone was triggered by the Kumamoto earthquake, but the fault zone has potential to generate an earthquake with larger slip that poses a high seismic risk in downtown Kumamoto area.

Keywords: 2016 Kumamoto earthquake, Active fault, Tectonic landform, Surface rupture, Kumamoto Plain, Suizenji fault zone, Digital elevation model

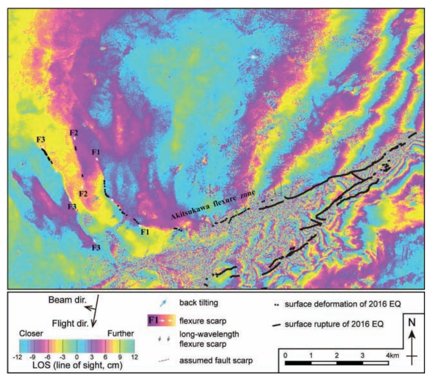

Figure 6

*Corresponding author: Hideaki Goto, hgoto@hiroshima-u.ac.jp

LETTER **Open Access**

Local site effects in Kumamoto City revealed by the 2016 Kumamoto earthquake

Seiji Tsuno*, Masahiro Korenaga, Kyosuke Okamoto, Hiroaki Yamanaka, Kosuke Chimoto and Takeshi Matsushima

Earth, Planets and Space 2017, **69**:37 doi:10.1186/s40623-017-0622-6
Received: 1 August 2016, Accepted: 28 February 2017, Published: 7 March 2017

Abstract

To evaluate local site effects in Kumamoto City, we installed six temporary seismic stations along a 6-km north–south survey line in the city immediately after the 2016 Kumamoto earthquake foreshock (Mj 6.4), which occurred on April 14, 2016. Seismic data from the 2016 Kumamoto earthquake (Mj 7.3), which occurred on April 16, 2016, were successfully recorded at two sites and indicated large amplitudes in the frequency range of 0.5–3 Hz. Site amplifications estimated from weak ground motion data, with a station at Mt. Kinbo used as a reference, are relatively variable along this survey line; however, site amplification factors in the frequency range of 0.5–3 Hz are not large enough to explain the amplitudes produced by the main shock. Nevertheless, site amplifications estimated from strong ground motion data recorded at the two sites during the main shock are large in the frequency range of 1–3 Hz. These findings reveal that the strong ground motions in the frequency range of 1–3 Hz were enhanced by nonlinear behavior of the subsurface soil in Kumamoto City. Moreover, it is observed that the frequency contents of the main shock data in the frequency range of 0.7–3 Hz differ significantly between the two sites, despite the proximity of these sites (600-m interval). Therefore, we also performed single-station microtremor measurements with an interval distance of approximately 100 m between these two sites. We confirmed that the peak frequencies of the horizontal-to-vertical spectral ratios of microtremors have trends that are similar to those of the site amplification factors between the two sites. However, these results could not explain the differences in strong ground motions observed at the two sites during the 2016 Kumamoto earthquake.

Keywords: Strong ground motion, Local site effect, Nonlinearity, Kumamoto City, 2016 Kumamoto earthquake

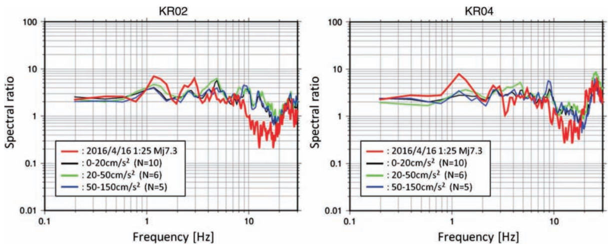

Figure 7

*Corresponding author: Seiji Tsuno, stsuno@rtri.or.jp

LETTER **Open Access**

Source process of the 2016 Kumamoto earthquake (Mj7.3) inferred from kinematic inversion of strong-motion records

Kunikazu Yoshida*, Ken Miyakoshi, Kazuhiro Somei and Kojiro Irikura

Earth, Planets and Space 2017, **69**:64 doi:10.1186/s40623-017-0649-8
Received: 1 August 2016, Accepted: 25 April 2017, Published: 3 May 2017

Abstract

In this study, we estimated source process of the 2016 Kumamoto earthquake from strong-motion data by using the multiple-time window linear kinematic waveform inversion method to discuss generation of strong motions and to explain crustal deformation pattern with a seismic source inversion model. A four-segment fault model was assumed based on the aftershock distribution, active fault traces, and interferometric synthetic aperture radar data. Three western segments were set to be northwest-dipping planes, and the most eastern segment under the Aso caldera was examined to be a southeast-dipping plane. The velocity structure models used in this study were estimated by using waveform modeling of moderate earthquakes that occurred in the source region. We applied a two-step approach of the inversions of 20 strong-motion datasets observed by K-NET and KiK-net by using band-pass-filtered strong-motion data at 0.05–0.5 Hz and then at 0.05–1.0 Hz. The rupture area of the fault plane was determined by applying the criterion of Somerville et al. (Seismol Res Lett 70:59–80, 1999) to the inverted slip distribution. From the first-step inversion, the fault length was trimmed from 52 to 44 km, whereas the fault width was kept at 18 km. The trimmed rupture area was not changed in the second-step inversion. The source model obtained from the two-step approach indicated 4.7×10^{19} Nm of the total moment release and 1.8 m average slip of the entire fault with a rupture area of 792 km^2. Large slip areas were estimated in the seismogenic zone and in the shallow part corresponding to the surface rupture that occurred during the Mj7.3 mainshock. The areas of the high peak moment rate correlated roughly with those of large slip; however, the moment rate functions near the Earth surface have low peak, bell shape, and long duration. These subfaults with long-duration moment release are expected to cause weak short-period ground motions. We confirmed that the southeast dipping of the most eastern segment is more plausible rather than northwest-dipping from the observed subsidence around the central cones of the Aso volcano.

Keywords: 2016 Kumamoto earthquake, Source process, Kinematic inversion, Near-fault strong motion

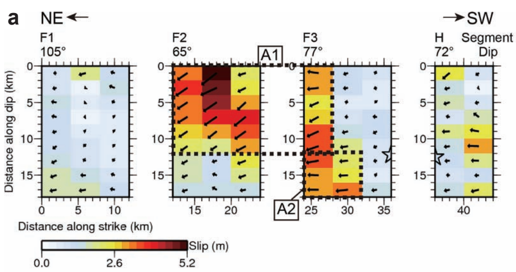

Figure 5

*Corresponding author: Kunikazu Yoshida, yoshida@geor.or.jp

LETTER Open Access

Effect of newly refined hypocenter locations on the seismic activity recorded during the 2016 Kumamoto Earthquake sequence

Tomoko Elizabeth Yano* and Makoto Matsubara

Earth, Planets and Space 2017, **69**:74 doi:10.1186/s40623-017-0656-9
Received: 10 August 2016, Accepted: 16 May 2017, Published: 30 May 2017

Abstract

We present the results of relocating 17,544 hypocenters determined from data recorded during the 2016 Kumamoto Earthquake sequence, during the interval between April 14, 2016, and August 31, 2016. For this, we used a double-difference relocation method to constrain high-resolution hypocenter locations by cross-correlation differential times as well as the NIED Hi-net catalog differential times. The sequence included two large events (on 14 April: M_{JMA}6.5 and on 16 April: M_{JMA}7.3) that occurred in a complicated region where the Hinagu and Futagawa faults meet. By comparing these high-resolution earthquake locations in three different periods [(P1) between 2001 and 2012; (P2) between M_{JMA}6.5 and M_{JMA}7.3; and (P3) between M_{JMA}7.3 and August 31, 2016], we present the significant seismicity after the mainshock relative to the background seismicity. Events during the Kumamoto Earthquake sequence occurred generally within the same sites of known faults and background seismicity. For an example, the seismicity during period P2 formed a sharp linear shape along the northern part of the Hinagu fault for about 20 km. A series of linear seismicity events occurred during period P3 along the Futagawa fault to the east (for about 28 km), in the northern part of the Aso caldera, and in the Oita region around the Beppu–Haneyama fault zone. These events also extended to the mid- and southern parts of the Hinagu fault zone and were shaped only after the *M*7.3 event. Moreover, high-resolution hypocenter locations also allowed us to identify some clusters of events that occurred in regions where background seismicity has not been confirmed. For instance, activity on the northwestern edge of the Aso caldera and in small areas within the Beppu–Haneyama fault zone became apparent with new seismic activity. We also demonstrate herein the absence of seismicity between the northeast extension of the Futagawa fault zone and the Aso caldera region, which became clearly shown after the *M*7.3 event. This low-seismicity region is located at the boundary of the low- and high-velocity structures and different focal mechanisms, but is also close to the maximum slip area of the *M*7.3 event.

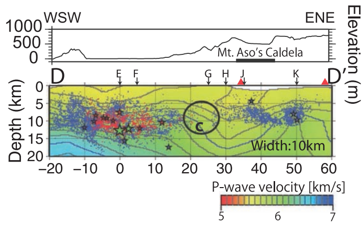

Figure 3

Keywords: The 2016 Kumamoto Earthquake, Double-difference method, Active fault zone, The Beppu–Shimabara graben

*Corresponding author: Tomoko Elizabeth Yano, tomoyano@gmail.com

Information for Contributors

General

1. Manuscripts should be submitted through the journal's Editorial Manager system (https://www.editorialmanager.com/epsp/default.aspx).
2. Only papers not previously published will be accepted, and the emphasis is on the originality of concept or observation.
3. Four varieties of article types are available.
   - 3.1 "Full papers" without word limit.
   - 3.2 "Express Letters" have a limit of 5000 words including the title page, abstract, keywords, main text, declarations, references, figure legends and table legends. The sum of the number of figures and tables should be less than or equal to 5.
   - 3.3 "Frontier Letters" can be submitted upon invitation by the Editor-in-Chief. "Frontier Letters" have a limit of 11,000 words including legends for figures and tables. One figure or table not exceeding one A4 page is counted as 500 words.
   - 3.4 "Technical reports" describe the technical development of instrument or software.
4. Authors retain the copyright, and distribution of articles is free under cc-by license.

Technical

1. Manuscripts should be written in English with double spacing.
2. Each manuscript should be organized in the following order: title, authors' names, affiliations, abstract, key words, main text, acknowledgement, appendix, references, and supplementary materials.
3. The corresponding author should be clearly indicated.
4. The abstract is limited to 300 words and should be informative and include principal findings and conclusions. Please avoid abbreviations.
5. The main text can have multiple free headings.
6. High-resolution figures should be provided in the following format; PDF (preferred format for diagrams), PNG (preferred format for photos or images), EPS ,TIFF, JPEG, BMP.
7. References must follow the Springer Basic style.

Correspondence

If you have any questions, please contact editorial@earth-planets-space.com.

A Grant-in-Aid for Publication of Scientific Research Results (251001) from Japan Society for the Promotion of Science is used for printing.

Continued from inside cover

Cover image: Asano, K. *et al*., *Earth, Planets and Space* 2016, **68**:147 DOI: 10.1186/s40623-016-0519-9

Continued from back cover

to be continued

Contents

Continued on inside back cover